geodiversitas

2021 • 43 • 1

A nearly complete skeleton of the oldest definitive erycine boid (Messel, Germany)

Krister T. SMITH & Agustín SCANFERLA

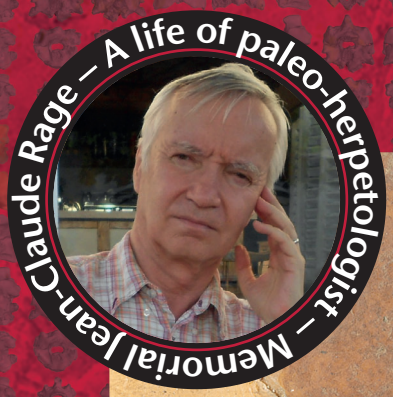

art. 43 (1) — Published on 14 January 2021
www.geodiversitas.com

PUBLICATIONS SCIENTIFIQUES

MUSÉUM NAL HIST NATURELLE

Geodiversitas est indexé dans / Geodiversitas *is indexed in:*
– Science Citation Index Expanded (SciSearch®)
– ISI Alerting Services®
– Current Contents® / Physical, Chemical, and Earth Sciences®
– Scopus®

Geodiversitas est distribué en version électronique par / Geodiversitas *is distributed electronically by:*
– BioOne® (http://www.bioone.org)

Les articles ainsi que les nouveautés nomenclaturales publiés dans *Geodiversitas* sont référencés par / *Articles and nomenclatural novelties published in* Geodiversitas *are referenced by:*
– ZooBank® (http://zoobank.org)

Geodiversitas est une revue en flux continu publiée par les Publications scientifiques du Muséum, Paris
Geodiversitas *is a fast track journal published by the Museum Science Press, Paris*

Les Publications scientifiques du Muséum publient aussi / *The Museum Science Press also publish:* ***Adansonia***, ***Zoosystema***, ***Anthropozoologica***, ***European Journal of Taxonomy***, ***Naturae***, ***Cryptogamie*** **sous-sections** ***Algologie***, ***Bryologie***, ***Mycologie, Comptes Rendus Palevol***

Diffusion – Publications scientifiques Muséum national d'Histoire naturelle
CP 41 – 57 rue Cuvier F-75231 Paris cedex 05 (France)
Tél. : 33 (0)1 40 79 48 05 / Fax : 33 (0)1 40 79 38 40
diff.pub@mnhn.fr / http://sciencepress.mnhn.fr

ISSN (imprimé / *print*) : 1280-9659/ ISSN (électronique / *electronic*) : 1638-9395

A nearly complete skeleton of the oldest definitive erycine boid (Messel, Germany)

Krister T. SMITH
Dept. of Messel Research and Mammalogy, Senckenberg Research Institute,
Senckenberganlage 25, 60325 Frankfurt am Main (Germany)
and Faculty of Biological Sciences, Institute for Ecology, Diversity and Evolution,
Max-von-Laue-Strasse 13, University of Frankfurt, 60438 Frankfurt am Main (Germany)
krister.smith@senckenberg.de

Agustín SCANFERLA
CONICET, Instituto de Bio y Geociencias del NOA (IBIGEO), 9 de Julio Nº 14 (A4405BBB),
Rosario de Lerma, Salta (Argentina)
and Dept. of Messel Research and Mammalogy, Senckenberg Research Institute,
Senckenberganlage 25, 60325 Frankfurt am Main (Germany)
agustin_scanferla@yahoo.com.ar

Submitted on 29 May 2019 | accepted on 8 November 2019 | published on 14 January 2021

urn:lsid:zoobank.org:pub:2FC06D0D-B51C-4E82-9B99-79E8B0EB05A7

Smith K. T. & Scanferla A. 2021. — A nearly complete skeleton of the oldest definitive erycine boid (Messel, Germany), *in* Steyer J.-S., Augé M. L. & Métais G. (eds), Memorial Jean-Claude Rage: A life of paleo-herpetologist. *Geodiversitas* 43 (1): 1-24. https://doi.org/10.5252/geodiversitas2021v43a1. http://geodiversitas.com/43/1

ABSTRACT
A nearly complete skeleton of an erycine boid is described from the Ypresian-Lutetian (early-middle Eocene) site of Messel, Germany, for which we propose the name *Rageryx schmidi* n. gen., n. sp. The animal had a total length of *c.* 52 cm, with *c.* 258 vertebrae. In skull proportions it is similar to ungaliophiine boids, especially *Ungaliophis*, and to *Tropidophis*. The proportions and distinctive accessory processes of the distal caudal vertebrae that are common to all living erycine boids are present in the specimen, although the processes are not as elaborate as in many extant species. The premaxilla was not protruded to form a wedge-shaped snout, and the nasofrontal joint does not appear to show any special buttressing, unlike in many burrowing snake species. Furthermore, the inner ear lacks adaptations to an actively burrowing mode of life. We conclude that the animal, while it was probably secretive, was not fossorial. Phylogenetic analyses using maximum parsimony and Bayesian inference place *Rageryx schmidi* n. gen., n. sp. unambiguously on the stem of the North American clade (*Lichanura* + *Charina*). If this relationship is accurate, it provides further support for a common Euro-American squamate fauna in the early Eocene. The majority of known Messel snake taxa are small-bodied with a small gape, suggesting that such forms may have played a greater role in the early evolutionary radiation of Booidea than their present diversity would suggest.

KEY WORDS
Boidae,
snakes,
Eocene,
Germany,
Messel,
biogeography,
new genus,
new species.

RÉSUMÉ
Le squelette presque complet du plus ancien boïdé éryciné avéré (Messel, Allemagne).
Le squelette presque complet d'un boïdé eryciné du site yprésien-lutétien (Éocène inférieur à moyen) de Messel, en Allemagne, est décrit. Nous proposons d'ériger pour lui le nouveau taxon *Rageryx schmidi* n. gen., n. sp. L'animal mesurait près de 52 cm de long, avec environ 258 vertèbres. Les proportions craniennes sont similaires à celles des boidés ungaliophiinés, en particulier *Ungaliophis* et *Tropidophis*. Les processus accessoires caractéristiques et les proportions des vertèbres caudales distales observés sur ce spécimen sont communes à tous les boidés erycinés actuels, bien que les processus ne soient pas aussi élaborés que chez beaucoup d'espèces vivantes. Le prémaxillaire n'est pas projeté en avant, ne donnant donc pas une forme en biseau au museau, et la suture nasofrontal n'est pas particulièrement renforcée, comme on peut le voir chez de nombreuses espèces de serpents fouisseurs. De plus, l'oreille interne ne présente pas les adaptations associées à un mode de vie fouisseur. Nous en concluons que cet animal n'était pas fouisseur, mais probablement très discret. L'analyse phylogénétique utilisant la méthode de parcimonie maximale et d'inférence bayésienne place *Rageryx schmidi* n. gen., n. sp. sans ambiguités en tant que groupe souche du clade nord-américain (*Lichanura* + *Charina*). Si ces liens de parentés sont corrects, le nouveau taxon apporte une preuve supplémentaire de l'existence d´une faune squamate commune entre l'Europe et l'Amérique pendant l'Éocène inférieur. La majorité des serpents fossiles de Messel sont de petite taille, avec une petite gueule. Ceci suggère que de telles formes ont pu jouer un role plus important, que leur présente diversité ne laisse à penser, dans la radiation évolutive initiale des Booidea.

MOTS CLÉS
Boidae,
serpents,
Éocène,
Allemagne,
Messel,
biogéographie,
genre nouveau,
espèce nouvelle.

INTRODUCTION

Erycines, or sand boas, are a distinctive group of smallish boid snakes with a broad distribution encompassing western North America, southeastern Europe, northern Africa, and central and southwest Asia (Hoffstetter & Rage 1972). These snakes share a number of morphological features (Bogert 1968; Hoffstetter & Rage 1972; Underwood 1976; Rieppel 1978a; McDowell 1979), some with the African *Calabaria reinhardtii* Schlegel, 1851, and are generally recovered as a clade in phylogenetic analyses of morphology (e.g., Kluge 1993; Gauthier *et al.* 2012; Scanferla *et al.* 2016). In contrast, molecular analyses usually find the North America taxa (*Lichanura* Cope, 1861 and *Charina* Gray, 1849) to be more closely related to the North American dwarf boa clade Ungaliophiinae (e.g., Wilcox *et al.* 2002), and Old World species (*Eryx*) to be more closely related to other boids in one way or another (e.g., Lawson *et al.* 2004; Noonan & Chippindale 2006; Pyron *et al.* 2013; Reynolds *et al.* 2014; Hsiang *et al.* 2015); a close relationship between *Eryx* Daudin, 1803 or erycines and the Oceanian *Candoia* Gray, 1842 was anticipated by Frazzetta (1975) and by Romer (1956), who may have been influenced by personal communications (McDowell 1979). The biogeographic signal apparent in the molecular data parallels that seen in several other cases of morphological-molecular incongruity in squamates (viz., the proposed clade *Anilius* Oken, 1816 + Tropidophiidae Brongersma, 1951 [Vidal *et al.* 2007; Pyron *et al.* 2013], the proposed clade *Calabaria* Gray, 1858 + Sanziniinae Romer, 1956 [Noonan & Chippindale 2006], the Neoanguimorpha-Paleoanguimorpha divergence [Vidal *et al.* 2012]) and makes the erycine problem a central one in snake evolution and biogeography.

Notwithstanding the current problems posed by erycines, they were among the first groups of modern snakes plausibly identified in the fossil record (Cope 1883). A plethora of fossil species, Paleocene through Pliocene in age, was attributed to the group over the course of the 20th century (Holman 2000), mostly described on basis of isolated trunk vertebrae. Yet, most of the reputed diagnostic features were not apomorphies, and erycine identity has one by one been stripped from most of the Paleogene species (Rage 1984; Szyndlar & Rage 2003; Smith 2013). Kluge (1993: 302) questioned whether any taxa based on isolated trunk vertebrae could confidently be attributed to erycines. The most recent reviews concluded that isolated vertebrae from the early Miocene of North America (Parham *et al.* 2012; Smith 2013) and the early Eocene of Europe (Szyndlar & Rage 2003) have the earliest apomorphic evidence for erycines. Paleontological evidence bearing on erycine origins and evolution is thus limited.

In this paper we describe a nearly complete skeleton of an undoubted erycine from the early-middle Eocene of the Messel Pit, Germany. The specimen represents the oldest record of an erycine for which a precise phylogenetic placement has been possible. Note that we use the term "erycines" in a loose sense to refer collectively to taxa previously regarded as belonging to the taxon Erycinae, viz. *Charina*, *Lichanura* and *Eryx*, as well as any fossils closely related to them. As noted above, there is grave concern about the monophyly of that taxon, but many of the adaptations shown by the living species are similar, so that it is a convenient shorthand, even if it ultimately might refer to a grade.

MATERIAL AND METHODS

The specimen was examined superficially by light microscopy and compared to the skeletons of extant booid snakes. Exam-

ined material: *Boa constrictor* Linnaeus, 1758 (CM 145331); *Calabaria reinhardtii* (SMF-PH 68); *Sanzinia madagascariensis* (Duméril & Bibron, 1844) SMF-PH 56; *Candoia carinata* (Schneider, 1801) (CM 118570, MBS 7103); *Charina bottae* (Blainville, 1835) (CM 36539, UMMZ 135016); *Eryx colubrinus* (Linnaeus, 1758) (MBS 447, SMF-PH 24); *Eryx conicus* (Schneider, 1801) (BM 1964.1224, CM 91863, SMF-PH 18); *Eryx jaculus* (Linnaeus, 1758) (Tü-VI.1935); *Eryx jayakari* Boulenger, 1888 (BM 1909.10.15.8); *Eryx johnii* (Russell, 1801) (BM 1930.5.8.31, SMF-PH 20); *Eryx muelleri* (Boulenger, 1892) (MBS 454); *Eryx tataricus* (Lichtenstein, 1823) (CM 145329); *Lichanura trivirgata* Cope, 1861 (CM 56093, CM 145332, SMF-PH 21). Additionally, the CT reconstructions at Digimorph were consulted (http://www.digimorph.org) as well as the available scanned boid species at MorphoSource (http://www.morphosource.org).

The skull and the tail of HLMD-Me 9723 were scanned using micro-computed tomography on a TomoScope HV 500 (Werth Messtechnik, GmbH) in an industrial µCT facility funded by the Wolfgang Pfeiffer Stiftung at the Technische Hochschule in Deggendorf, Germany. Parameters for head scan: 150 mA, 165 kV, 1600 steps, no binning or drift correction, voxel resolution 12.68 µm. Parameters for tail scan: 250 mA, 165 kV, 1600 steps, no binning or drift correction, voxel resolution 20.22 µm. The volume files were analyzed using VG Studio MAX v3.2 on a high-end computer workstation at Senckenberg. The 3D surface models in the supplementary figures are surface determinations exported as STL meshes from VG Studio, converted to U3D in MeshLab (Cignoni *et al.* 2008), and typeset in LaTeX.

To elucidate the phylogenetic relationships of the fossil, it was scored for a modified version of the Scanferla *et al.* (2016) matrix. The matrix was expanded with characters taken from papers on erycine or booid anatomy (Underwood 1976; Rieppel 1978a; Kluge 1993; Cundall & Irish 2008; Gauthier *et al.* 2012; Smith 2013) and others discovered during the present study. New taxa scored include *Eryx conicus*, *Charina bottae*, *Candoia carinata*, *Sanzinia madagascariensis* as well as the fossil taxa *Ogmophis compactus* Lambe, 1908 and *Calamagras weigeli* Holman, 1972 based on the referred specimens of Smith (2013). The final matrix comprises 207 characters and 42 taxa. Multistate characters that were considered additive (25 in total) were ordered.

The matrix was subjected to maximum parsimony (MP) analysis in PAUP* v. 4 (Swofford 2003) using a heuristic search with TBR branch-swapping and 100 random addition-sequence replicates. To assess support, 1000 bootstrap pseudoreplicates were conducted, but since a single island of most-parsimonious trees was hit 100% in the heuristic search, the "fast" addition-sequence option was selected here. A second analysis used the well-supported (bootstrap > 50% and posterior probability > 95%) nodes in the molecular tree of Reynolds *et al.* (2014) as a topological constraint (backbone) to assess robustness of fossil placement in the face of morphological-molecular incongruity (see Parham *et al.* 2012).

We also conducted analyses using standard Bayesian inference (BI) and BI that made use of the fossilized birth-death model (Stadler 2010) as implemented in MrBayes v3.2 (Ronquist *et al.* 2012). For the latter, the ingroup was constrained to be monophyletic. Since the age of most fossil taxa in our matrix is not very precisely known below the level of stage, we took calibrations for most fossil taxa to be a uniform distribution between respective stage boundaries (Gradstein *et al.* 2012). Exceptions were taxa known from Messel (see Lenz *et al.* 2015 on age) and the Medicine Pole Hills (see Smith 2011 on age). Generally flat priors were assumed (Matzke & Wright 2016; Zhang *et al.* 2016). We assumed a diversified sampling strategy, as the matrix was designed to cover major lineages outside of Caenophidia, with a low sampling probability. The tree age prior (age of the ingroup) was taken to be an offset exponential distribution with a minimum age of 93.9 Ma (oldest definitive snakes; but see also Caldwell *et al.* 2015) and a mean of 145 Ma (the Jurassic-Cretaceous boundary). Similarly, a second analysis utilizing minimal molecular topological constraints (*Xenopeltis* + *Loxocemus* + Pythonidae, *Loxocemus* + Pythonidae, Boidae + *Eryx* + *Candoia*, Charinidae, Amerophidia) based on Reynolds *et al.* (2014), as above, was conducted. In all analyses using BI, the first 5000 trees (25%) were discarded as burn-in (see Appendix 2).

ABBREVIATIONS

BM	British Museum (Natural History), London;
CM	Carnegie Museum of Natural History, Pittsburgh;
HLMD-Me	Messel collection, Hessisches Landesmuseum, Darmstadt;
MBS	Naturhistorisches Museum, Basel;
SMF-PH	Paleoherpetology collection, Senckenberg Research Institute, Frankfurt am Main;
Tü	Comparative osteology collection, University of Tübingen;
UMMZ	University of Michigan Museum of Zoology, Ann Arbor.

GEOLOGICAL SETTING

The specimen, HLMD-Me 9723, was collected on 5 August 1987, at HLMD excavation site 16b in the Messel Pit, a UNESCO World Heritage site near Frankfurt am Main (Smith *et al.* 2018). The deposits represent a maar lake that formed following phreatomagnatic eruptions around 48.2 Ma (Lenz *et al.* 2015). The specimen comes specifically from the Middle Messel Formation, a dark algal mudstone, with fine-scale laminations (0.14 mm) interpreted as annual layers (Goth 1990). Each lamina comprises a clay-rich (montmorillonite, smectite family) layer, thought to be derived from particles washed in during the dark half of the year, and an algal-rich (mostly *Tetraedron minimum*), thought to be derived from annual blooms during the light half of the year (Goth 1990; Weber 1991). With average layer thickness and the height of the excavation horizon above the base of the Middle Messel Formation, the time represented by the Middle Messel Formation is readily calculated. However, the lowest part of the crater fill comprises volcanic breccia and coarse clastic sediments that represent an unknown interval of time. Astronomically tuned pollen profiles suggested two plausible ages

for the marker bed Alpha (Lenz *et al.* 2015). Since an exact distance between the horizon of discovery and Alpha cannot be given in any case, we can only say that the specimen is latest Ypresian or earliest Lutetian in age.

SYSTEMATIC PALEONTOLOGY

Suborder SERPENTES Linnaeus, 1758
Infraorder ALETHINOPHIDIA Nopcsa, 1923
Superfamily BOOIDEA Gray, 1825 *sensu* Gauthier *et al.* (2012)

Genus *Rageryx* n. gen.

urn:lsid:zoobank.org:act:22B713C0-B9BD-469A-B852-A8D9CEB9E40F

TYPE SPECIES. — *Rageryx schmidi* n. sp.

KNOWN DISTRIBUTION. — As for type and only known species.

ETYMOLOGY. — After the late Jean-Claude Rage, in recognition of his lifelong contributions to paleoherpetology, and the fact that some of his earliest work was on erycines.

DIAGNOSIS. — As for type and only known species.

Rageryx schmidi n. gen., n. sp.
(Figs 1; 2A-C; 3A-E; 4A-D; 5A-C; 6A-C; 7A, B; 8A-D; 9A-D; 10A-D; 11B-E; Appendix 1: Figs S1-S8)

urn:lsid:zoobank.org:act:AEB68284-BF3F-4980-8CD3-960415C732E0

HOLOTYPE AND ONLY KNOWN SPECIMEN. — HLMD-Me 9723, nearly complete skeleton.

TYPE LOCALITY. — Early or middle Eocene (MP 11, Ypresian or Lutetian) of the Middle Messel Formation, Germany. Known only from type locality.

ETYMOLOGY. — After Dietmar Schmid, past president of the Senckenberg Gesellschaft für Naturforschung, in recognition of his estimable service to the society.

DIAGNOSIS. — Small boid snake with the following unique combination of characters: skull with short snout and moderately extensive braincase; orbits located in front of longitudinal midpoint of skull; anterior margin of premaxilla in line with arch defined by maxillae; nasal process of premaxilla small but distinct, with flat anterior face; maxillary tooth count around 16; maxilla with small posteromedial flange for ectopterygoid; prefrontal with anterolateral lamina and medial and lateral footprocesses; frontal table trapezoidal; parietal with low mid-sagittal ridge on posterior third; parasphenoid rostrum triangular with very broad base and weak, posterior ventral midline ridge; right Vidian canal larger than left; shelf bounding groove for posterior opening of Vidian canal obscures foramen for palatine branch of cranial nerve VII; supraoccipital significantly exposed externally; free end of supratemporal short; quadrate ramus of pterygoid with longitudinal, dorsally open groove; palatine ramus of pterygoid long; ectopterygoid straight with simple anterior end; coronoid present but reduced, lacking a distinct anteromedial process; compound bone with gradual decay of coronoid eminence anteriorly, and low, straight prearticular crest; about 220 precloacal and 38 caudal vertebrae; mid-trunk vertebrae with low and short neural spine; posterior trunk vertebrae without depressed neural arch; caudal neural spines relatively thick but not bifurcated; neural arch in middle of tail vaulted with flat, vertical posterior surface; distal caudal vertebrae short and tall (much taller than long); supernumerary process of caudal vertebrae present at least in rudimentary form, viz., pterapophyses present on majority of caudals, small postzygapophyseal wings and posterior extensions of the prezygapophysis present; and zygosphene-zygantral articulations present on distal caudal vertebrae.

REMARKS

Three erycine taxa have been named from the Eocene of Europe, *Calamagras gallicus* Rage, 1977, *Cadurceryx filholi* Hoffstetter & Rage, 1972 and *Cadurceryx pearchi* Holman, Harrison & Ward, 2006. The first is known from much of the Ypresian (early Eocene), from MP 8+9 to MP 10 (Rage 1977, 2012). The second is known possibly as early as MP 13 and certainly from MP 16 to MP 19+20 (Hoffstetter & Rage 1972; Rage 1984, 2012, 2013). The third is described only from the late Eocene Headon Hill Formation of England. The Middle Messel Formation, considered to be MP 11 (Franzen 2005), falls in-between and straddles the Ypresian-Lutetian boundary (Lenz *et al.* 2015).

Smith (2013) found that *Calamagras weigeli* from the late Eocene of North America is closely related to Ungaliophiinae, a result confirmed here. He also found that the type species of *Calamagras* Cope, 1873, *Cal. murivorus* Cope, 1873 from the early Oligocene, shows similarity of proportions to *Cal. weigeli*, and even if a lack of referred material with diagnostic characters (absence of hemapophyses on all caudal vertebrae; see Smith 2013) currently prevents a critical appraisal of its relationships, it is not unlikely that *Cal. murivorus* will also turn out to be related to Ungaliophiinae. Thus, the genus name *Calamagras* cannot be used for HLMD-Me 9723.

Cadurceryx filholi, in contrast, is a highly derived species in which the accessory processes are not only more highly developed but also extend far into the trunk. This unusual morphology is not seen in any living erycine. Furthermore, *Cad. filholi* shows a very depressed neural arch on posterior trunk vertebrae, a derived character that it shares with extant *Eryx* (and also Charininae) and that distinguishes it from the vaulted neural arch of HLMD-Me 9723. Whatever its precise phylogenetic relations, *Cad. filholi* is clearly not closely related to HLMD-Me 9723, and the name *Cadurceryx* cannot be applied to the specimen.

Cadurceryx pearchi, finally, is known exclusively from caudal vertebrae (Holman *et al.* 2006). The two diagnostic features of *Cad. pearchi* with respect to *Cad. filholi*, according to the authors, were the size of the cotyle (larger than neural canal) and the presence of a 'tubercle' on the anterior end of the prezygapophysis. The tubercle was not labelled, but if we understand it correctly, it is absent in *Rageryx schmidi* n. gen., n. sp. The size of the cotyle with respect to the neural canal appears to be variable in the

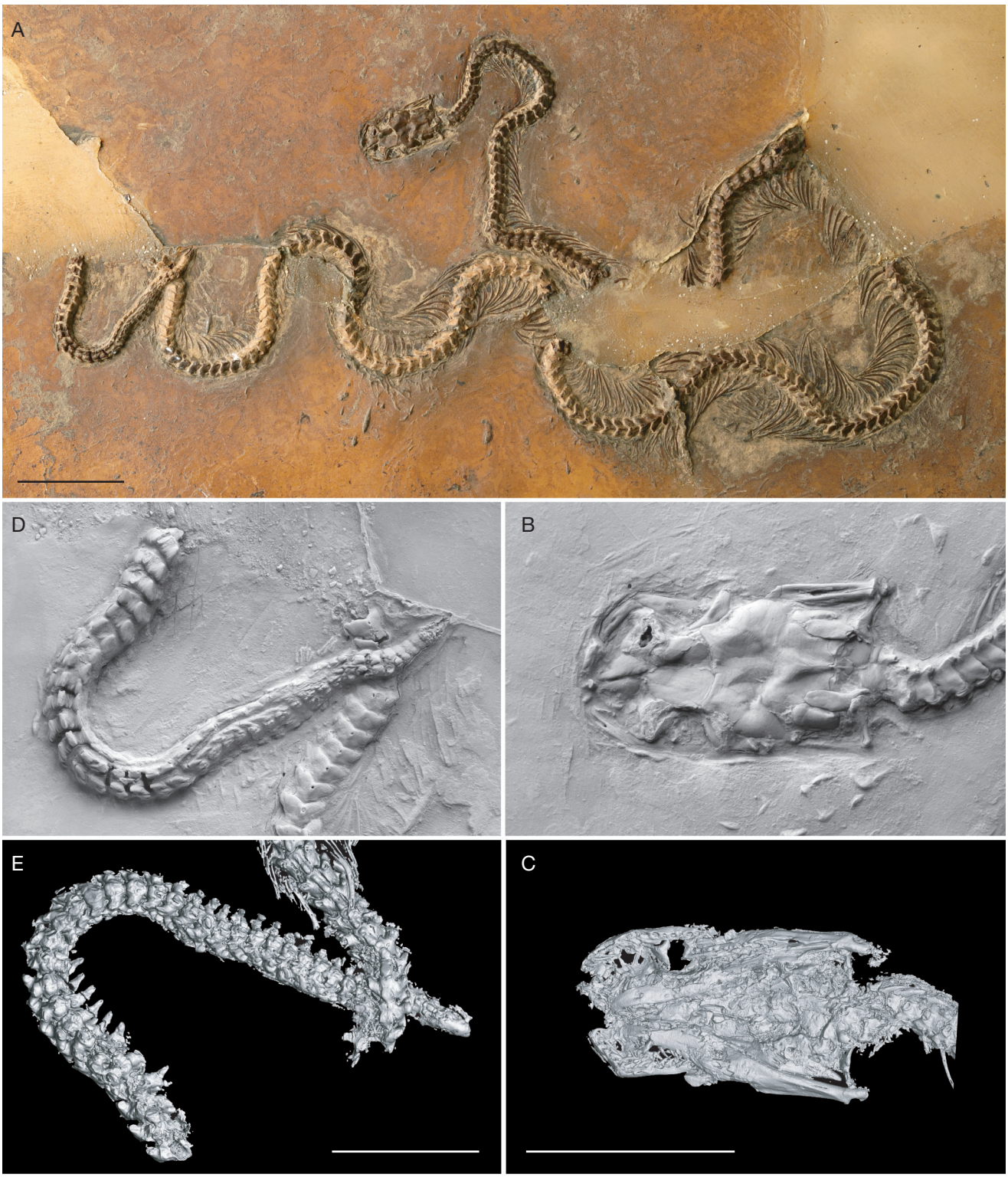

Fig. 1. — HLMD-Me 9723, holotype of *Rageryx schmidi* n. gen., n. sp.: **A**, photograph of whole specimen; **B**, photograph of skull (coated with ammonium chloride) in dorsal view; **C**, 3D rendering of skull, based on CT scan, in ventral view; **D**, photograph of tail (coated with ammonium chloride) in roughly dorsal view; **E**, 3D rendering of tail, based on CT scan, in roughly ventral view. Scale bars: A, 2 cm; B-E, 1 cm.

type series of *Cad. pearchi* (Holman *et al.* 2006: figs. 2a, d and 3a, e), potentially as a result of vertebral position or intraspecific variation, calling into question the validity of this diagnostic feature. There are additional differences between *Cad. pearchi* and *R. schmidi* n. gen., n.sp, such as caudal vertebrae being taller than wide and having a more vaulted neural arch. Thus, there is no reason to consider that these two species are closely related.

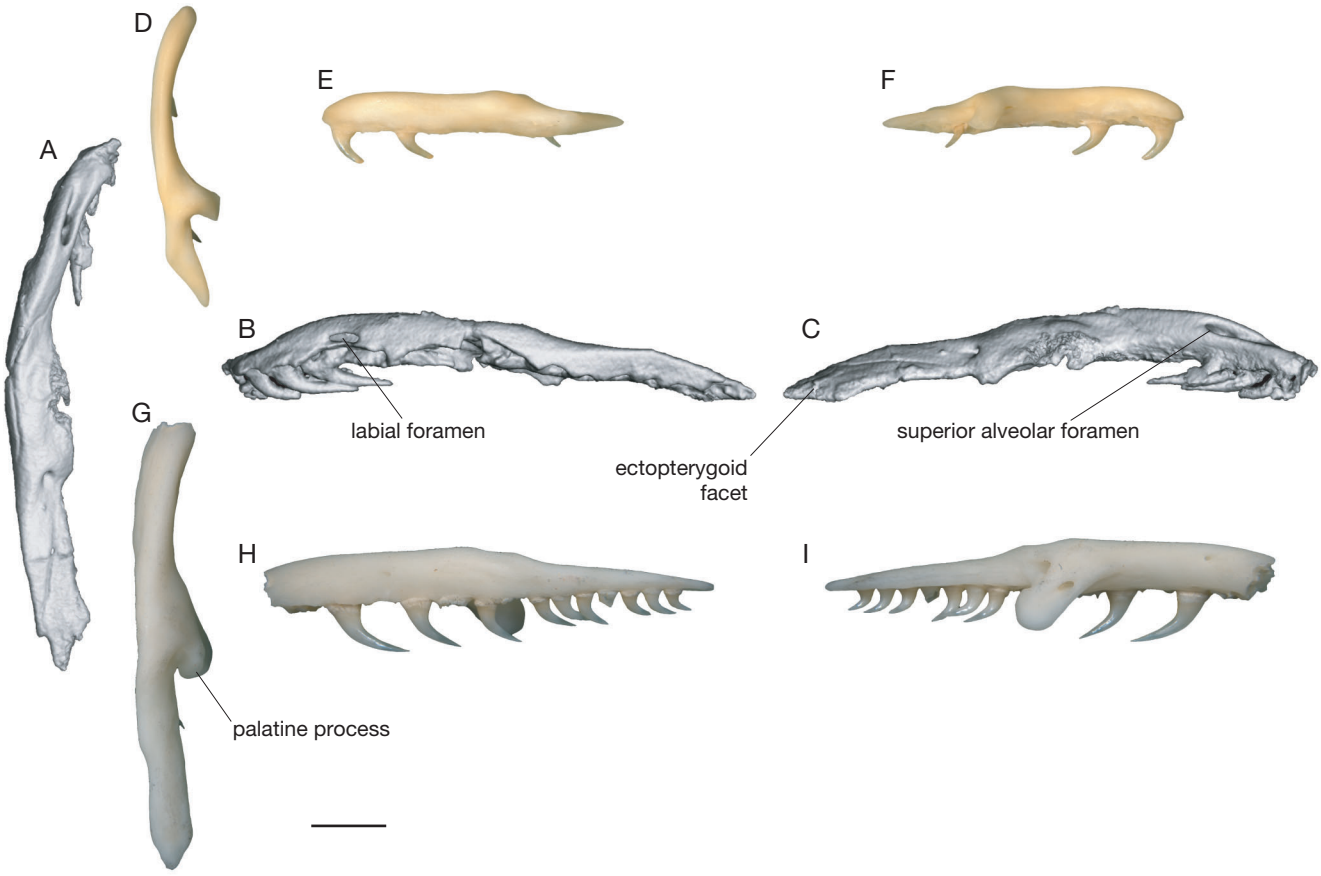

Fig. 2. — Maxilla: **A**-**C**, left maxilla of HLMD-Me 9723, holotype of *Rageryx schmidi* n. gen., n. sp., in dorsal, lateral and medial views, respectively; **D**-**F**, left maxilla of *Eryx jaculus* (Tü-VI.1935) in dorsal, lateral and medial views, respectively; **G**-**I**, left maxilla of *Lichanura trivirgata* (CM 145332) in dorsal, lateral and medial views, respectively. Scale bar: A-C, 1 mm; D-I, 2 mm.

The question now arises whether *Rageryx* n. gen. is the appropriate generic name for "*Calamagras*" *gallicus*. Rage (1977) stated that small pterapophyses are present in the holotype caudal vertebra, MNHN GR 7896, but other accessory processes are absent. It is remarkable, therefore, to find more of them present in *Rageryx schmidi* n. gen., n. sp., a younger European taxon. However, as noted in the description, it is the pterapophyses that occur most proximally in HLMD-Me 9723. Therefore, MNHN GR 7896 might derive from a more proximal part of the tail where the other processes do not occur. On the other hand, its proportions speak for a more distal position in the caudal series. MNHN GR 7896 also appears to have more bulbous processes than HLMD-Me 9723. With regard to the shape of the neural spine, HLMD-Me 9723 and referred trunk vertebrae of "*Cal.*" *gallicus* appear to be fully comparable. A clear resolution of this taxonomic problem will have to await the discovery and description of further caudal material from the Ypresian of France, preferably from the type locality, i.e., Grauves in the Paris Basin.

Given the distinctiveness and relatively early occurrence of *Cadurceryx* in Europe (Rage 2012), one hypothesis is to derive it from "*Calamagras*" *gallicus* or *Rageryx schmidi* n. gen., n. sp. (or a closely related form). A second hypothesis is that it represents an early dispersal of a taxon more closely related to *Eryx* into Europe. Cranial remains of these fossils apart from Messel are meager, and there are no fossils, at present, from MP 12 (Rage 2012). Consequently the data are insufficient to determine the relationships of *Cad. filholi*.

Description

HLMD-Me 9723 is a nearly complete skeleton, highly contorted and missing four sections of the axial skeleton (Fig. 1A). It is preserved on three plates that had been broken during excavation and rejoined. Because of the missing sections, the total length of the animal can only be given as *c.* 52 cm. A counterpart is not present in the HLMD collections.

The orbits are located in front of the longitudinal midpoint of the skull (Fig. 1B; Appendix 1: Fig. S1). The skull on the whole shows a short snout and moderately extensive braincase. Thus the general proportions of the skull are similar to ungaliophiine boids, especially *Ungaliophis* Müller, 1880, and to *Tropidophis* Bibron *in* Ramon de la Sagra, 1840 (Cundall & Irish 2008: fig. 2.62 and 2.65). They differ both from the primitive alethinophidian pattern, in which the elongate braincase is narrow anteriorly but widened at the otic capsule, and from most erycines, in which the braincase behind the orbit is shortened (Cundall & Irish 2008).

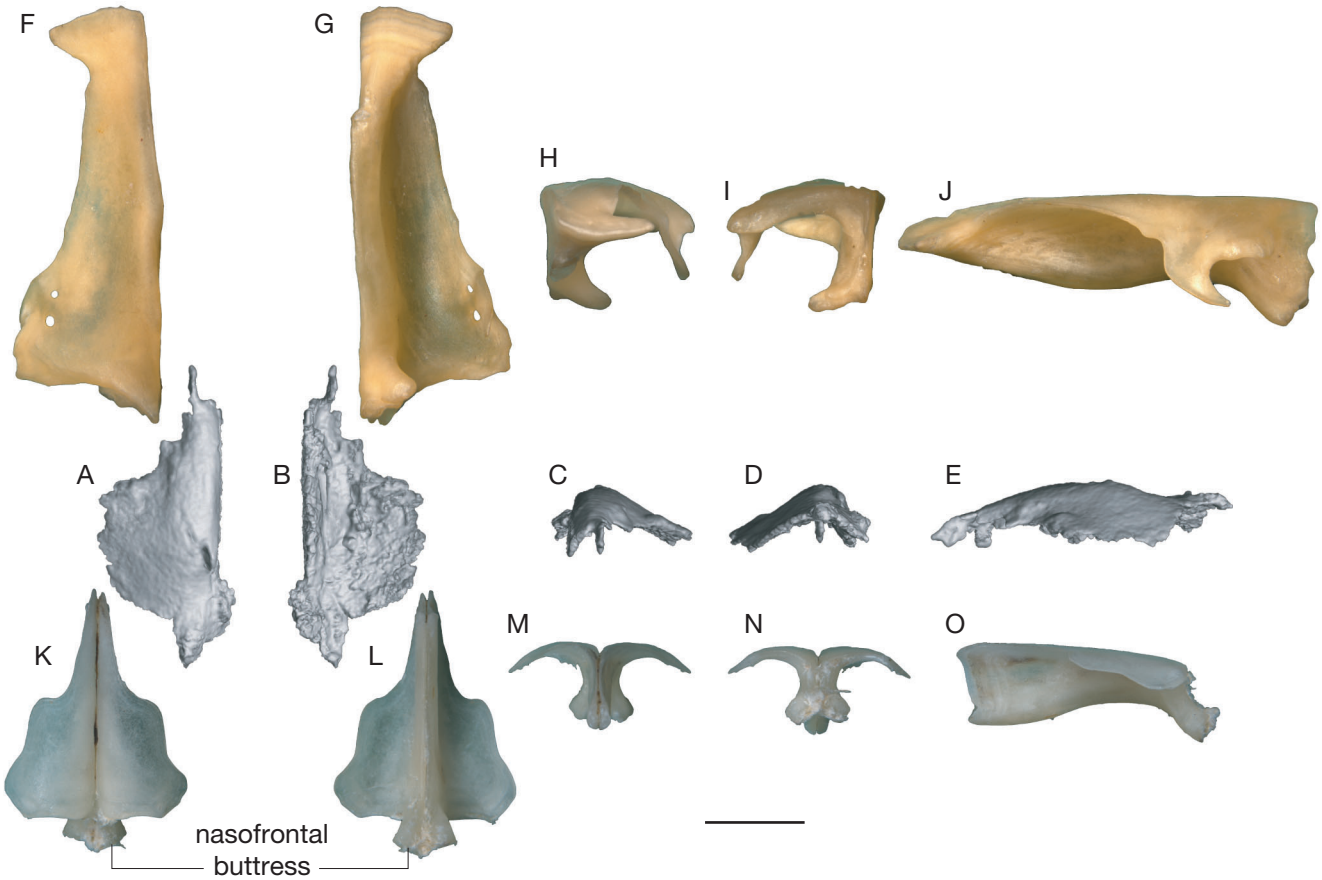

FIG. 3. — Nasal: **A**-**E**, left nasal of HLMD-Me 9723, holotype of *Rageryx schmidi* n. gen., n. sp., in dorsal, ventral, anterior, posterior, and lateral views, respectively; **F**-**J**, left nasal of *Eryx johnii* BM 1930.5.8.31 in dorsal, ventral, anterior, posterior, and lateral views, respectively; **K**-**O**, united left and right nasals of *Lichanura trivirgata* CM 145332 in dorsal, ventral, anterior, posterior, and lateral views, respectively. Scale bar: A-E, 1 mm; F-O, 2 mm.

Like those of several adult boid skulls examined, the posterior region of the parietal bone of HLMD-Me 9723 is clearly projected posteriorly, especially the supratemporal processes. This posterior projection overlaps the anterodorsal edge of the supraoccipital, like in adult individuals of large and small boids and macrostomatans in general (e.g., Smith & Scanferla 2016). Also, the well-preserved tips of the neural spines of the trunk vertebrae show well-finished caps of bone. Taken together, these anatomical traits present in the parietal bone, and the advanced state of ossification observed in skull and trunk vertebrae, evidence that HLMD-Me 9723 represents an adult postnatal ontogenetic stage. Thus, the species it represents was apparently smaller than typical adult Rosy Boas (*Lichanura trivirgata*, length 43-112 cm), and many adult Rubber Boas (*Charina bottae*, length 35-84 cm) (Stebbins 2003). HLMD-Me 9723 is also smaller than many *Eryx*. *Er. johnii* and *Er. tataricus* are the largest of the genus, with total length in large individuals >1 m, but all other species are smaller (Seufer 2001).

Premaxilla

The premaxilla is only partially preserved, yet there is every indication that its anterior margin was in line with the curvature of the arch defined by the maxillae (Fig. 1B, C). Thus, it was not produced far forward, unlike in extant erycines, *Loxocemus bicolor* Cope, 1861 and *Calabaria reinhardtii*. A small, ovate nasal process is present that projects posterodorsally and has a flat anterior surface that would have been visible externally between the nasal bones. It is similar to that of many boids and totally unlike the low crest completely hidden between the nasal bones in *Eryx* (Cundall & Irish 2008).

Maxilla (Fig. 2; Appendix 1: Fig. S2)

The maxilla is elongate, slightly dorsally arched element (Fig. 2A-C). Its anterior end is most notable for a large dorsal foramen (superior alveolar foramen, s.a.f.) continued anteriorly by a deep groove. This foramen is most comparable to that in *Charina bottae*, which, however, is disposed more laterally. It presumably transmits the subnarial artery and superior alveolar nerve onto the snout, but the reasons for its large dimensions are unknown. A weak ascending process begins to rise adjacent to the groove and terminates at the level of the superior alveolar foramen and palatine process (pl.pr.); it is more strongly developed than in *Lichanura trivirgata* (Fig. 2H, I), but not as strong as in *Ch. bottae*. The lateral surface of the bone is pierced by a single, elongate labial foramen (l.f.), which transmits branches of the maxillary artery and superior alveolar nerve. A small facet, probably for the prefrontal, is present medial to the ascending process.

The dorsal surface of the posterior end of the maxilla appears to show several fine, longitudinal striae (Fig. 2A), whose origin may lie with the ectopterygoid articulation. The palatine process is poorly preserved, and little can be said of its size, orientation, and morphology; however, it appears to have been asymmetrical, with a steep posterior margin and a probably more gradual anterior margin. Presumably the palatine process was pierced by a foramen, as in other boids. A single foramen is visible on the dorsal surface at the level of the posterior margin of the palatine process, as in other boids (Fig. 2D, G).

Nasals (Fig. 3; Appendix 1: Fig. S3)
The elongate nasals are gently dorsally convex in sagittal and transverse planes (Fig. 3C-E). They contact one another on the midline for most of their length. Each comprises a plate posteriorly over the nasal capsule (the horizontal lamina) and a long, slightly thickened anteromedial process (Fig. 3A, B). All examined *Eryx* also have a strong horizontal expansion of the anterior end of the horizontal lamina (Fig. 3F-H), which is lacking in *Lichanura trivirgata* (Fig. 3K-N) and other boids. The anteromedial processes curve ventrally to contact the nasal process of the premaxilla, which slightly separates them at their distal end. An anterolateral process, as in *Boa* Linnaeus, 1758, is lacking. Posterolaterally the nasal is overlapped by the prefrontal, as in *Li. trivirgata* and *Charina bottae* but unlike in *Eryx* (Rieppel 1978a; Cundall & Irish 2008). The posterolateral end of the nasal is squared off, but posteromedially there appears to be a posterior expansion; due to the tightly apposition of the frontal in this region, the true morphology is uncertain. A triangular, posteromedial prong extending posteriorly between the frontals was present in all examined *Eryx* but is lacking in *Li. trivirgata* and *Ch. bottae*. (In *Boa* and *Candoia carinata*, the nasals taper posteriorly and so they necessarily form a triangular point, but there is no anteromedian notch in the frontal; rather the space is occupied by the prefrontal. Thus, such a prong can be regarded as absent in these taxa.) There is no evidence of a vertical buttress that would have articulated with the lateral (subolfactory process) or medial pillars of the frontal at the prokinetic joint, unlike in extant erycines (Fig. 3I, J, N, O) as well as some other fossorial forms (Rieppel 1978a; b; pers. obs.), but it is likely that the nasal contacted the frontal beneath the olfactory tracts, as in most constrictors. All examined *Eryx* have one or two foramina through the posterolateral corner of the nasal, although it is uncertain what structures pass through it; these foramina are lacking in HLMD-Me 9723 and other boids.

Prefrontal (Appendix 1: Fig. S4)
On the whole, both elements are poorly preserved. A large anterolateral lamina is present (Fig. 1B), unlike in *Eryx*. The triangular dorsomedial projection of this lamina that extends medially behind the nasals toward the contralateral element is comparable in extent to Charininae; the prefrontals do not meet one another on the midline. The orbital lamina forms the anterior wall of the orbit. The medial foot-process is well developed and curves slightly laterally. The prefrontal is complete enough to deduce that the lateral foot-process was less well developed, more like *Boa constrictor* than the larger process of *Eryx*, Charininae and *Calabaria reinhardtii*. A small foramen of unknown significance pierces the ventral margin of the bone in the embayment between the two foot-processes.

Frontal (Fig. 4; Appendix 1: Fig. S5)
The smooth frontal table is trapezoidal, with a long medial, shorter and slightly concave lateral, and oblique anterior and posterior margins (Fig. 4A). Consequently there is no deep median notch between the frontals for reception of the nasals. In this it differs from the parallelgram-shaped table of *Eryx* (Fig. 4E). It appears that a small foramen exits dorsally through the posterolateral corner. The anterolateral margin is smooth and lacks a distinct notch for the prefrontal, unlike in *Lichanura trivirgata* (Fig. 4I). A prominent supraorbital shelf, as in Boinae, is absent (Fig. 4B, C). The posterolateral corner has a postolateral projection for accomodating the anterolateral corners of the parietal dorsally (Fig. 4A, D), like in *Eryx* (Fig. E, H) but unlike in Boinae and *Li. trivirgata* (Fig. I, L). A small facet for articulation of the postorbital may be present.

The ventral portion of the frontals is almost certainly present but could not be distinguished due to crushing. Thus, the extent and morphology of the medial and lateral frontal pillars and the posteroventral projection bounding the optic foramen cannot be ascertained.

Postorbital (Appendix 1: Fig. S6)
The dorsal portion shows an elongate facet where it articulated along the parietal and, anteriorly, a small part of the frontal (Fig. 1B). It tapers strongly ventrally, so that the postorbital process is thin, unlike in Boinae and some *Eryx* (e.g., *Er. colubrinus*). The process is broken, so that its ventral extent is uncertain, but comparison of the left and right elements suggests that it was less extensive than in most booids. The preserved portion shows no evidence of a posterior deflection, as is present in *Candoia carinata* and many *Eryx* (e.g., *Er. colubrinus, Er. conicus, Er. jayakari* and *Er. tataricus*, but not *Er. jaculus*).

Parietal
The parietal bone is relatively broad, only slightly longer than wide (Fig. 1B). Its widest point is found anterior to mid-length, well in front of the otic capsules. The anterior margin is shallowly concave except at the midline, where a small process projects between the frontals. The dorsal surface of the anterior part of the parietal is flat, and a low mid-sagittal ridge is developed only in about the posterior one-third of the bone. In this respect it is similar to *Lichanura*, *Charina* and Ungaliophiinae and differs from *Eryx* and Boinae, in which the sagittal crest is sharper and far more extensive (Cundall & Irish 2008). The ventral extent of the parietal forming the lateral wall of the braincase is almost certainly present, but could not be distinguished due to crushing.

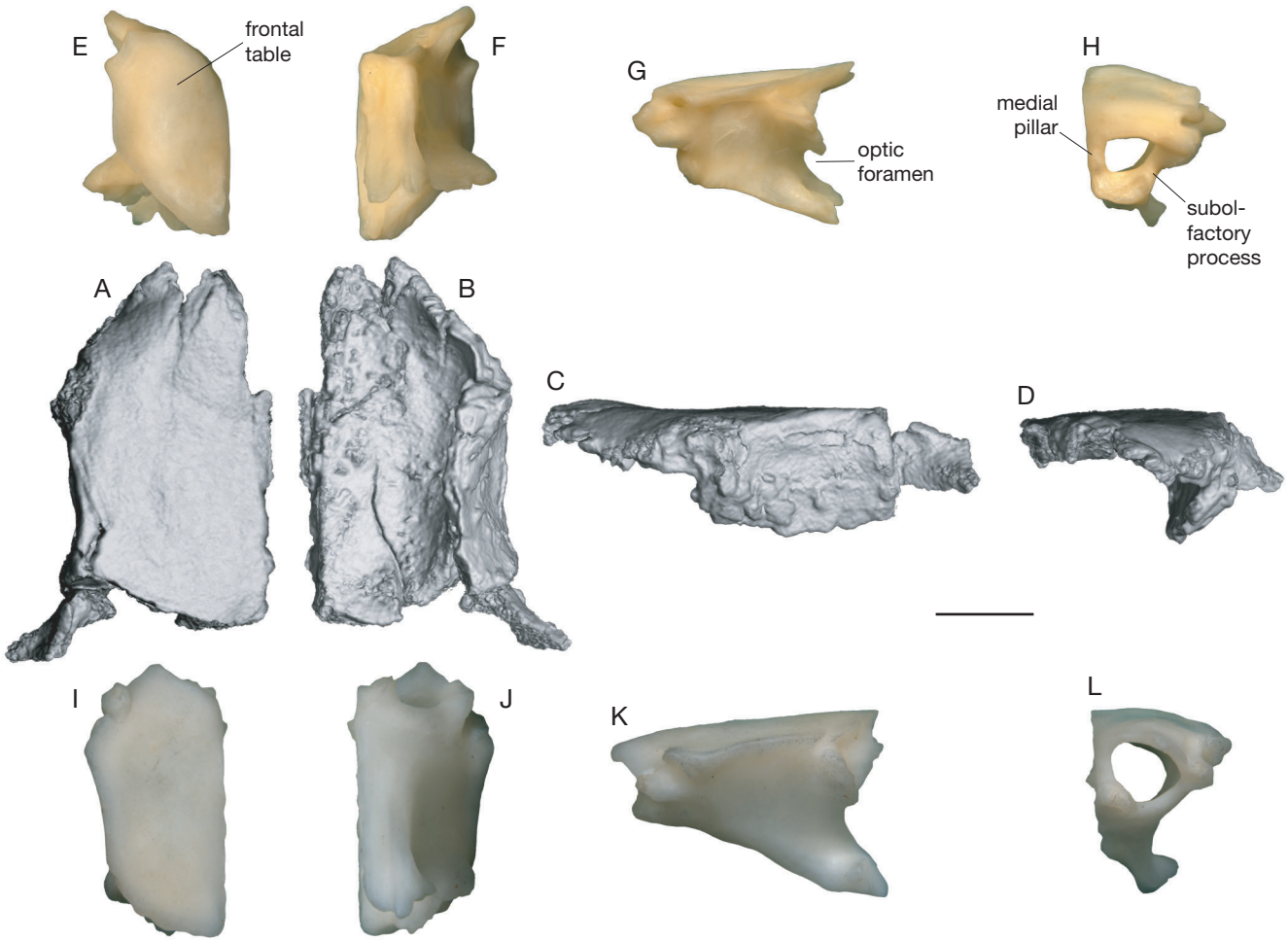

Fig. 4. — Frontal: **A**-**D**, left frontal of HLMD-Me 9723, holotype of *Rageryx schmidi* n. gen., n. sp., in dorsal, ventral, lateral, and anterior views, respectively; **E**-**H**, left frontal of *Eryx johnii* BM 1930.5.8.31 in dorsal, ventral, lateral, and anterior views, respectively; **I**-**L**, left frontal of *Lichanura trivirgata* CM 145332 in dorsal, ventral, lateral, and anterior views, respectively. Scale bar: A-D, 1 mm; E-L, 2 mm.

Parabasisphenoid ("sphenoid" of Cundall & Irish 2008) (Fig. 5; Appendix 1: Fig. S7)

This is a triangular element with a broad, regularly tapering rostrum (Fig. 5A, B). The rostrum is broader relative to the width of the basisphenoid portion of the bone than in any examined constrictor. Its dorsal surface is weakly concave in transverse section (Fig. 5A). Its ventral surface is nearly flat proximally, but distally there is a ventral keel formed beyond the terminus of the cristae trabecularis. On the main body of the basisphenoid portion there is a weak, midline ridge, similar to that seen in some constrictors, like *Loxocemus bicolor*, *Lichanura trivirgata,* and *Candoia carinata*, but no indication that the ridge bifurcates anteriorly, as it does in *Lo. bicolor* (Smith 2013) and *Li. trivirgata* (Fig. 5H).

In dorsal view the sella turcica – dorsal margin of the dorsum sella or pituitary fossa – is approximately in line with the greatest lateral extent of the bone, but crushing has nearly obliterated the fossa. It appears that the badly crushed parasphenoid wings are strong with a well-developed articulation for the parietal articulation, but their exact extent cannot be determined. If our interpretation is correct, these project more strongly than any observed in extant constrictors, except *Candoia carinata*, where they are also anteroposteriorly longer. Neurovascular foramina are difficult to distinguish in the CT scan. The right egress for cranial nerve VI, however, appears to be present at approximately the level of the lateral margin of the pituitary fossa. Assuming mirror symmetry for the left egress, the foramina would be widely spaced, like in *Lichanura trivirgata* (Fig. 5G) and most examined snakes but unlike in *Loxocemus bicolor* (Smith 2013), some *Eryx* [e.g., *Er. johnii* (Fig. 5D), *Er. tataricus*] and *Candoia carinata*. The right Vidian canal is distinctly larger than the left one, as in Boidae (Underwood 1976).

Prootic (Fig. 6)

The opening for the maxillary ramus of the trigeminal nerve (V2) is presumably situated between the prootic and the parietal, with the prootic deeply notched for the nerve, but the notch is not distinct on either side (Fig. 6A). The opening for the mandibular ramus (V3) is located posteriorly. In most boids (Fig. 6D, G) these foramina are separated by an ophidiosphenoid (sensu Gauthier *et al.* 2012), but it is lacking in *Eryx colubrinus*, *Er. jaculus*, *Er. muelleri*, and *Er. tataricus* (among examined *Eryx*); the region is too damaged to be certain in HLMD-Me 9723. The hyomandibular branch

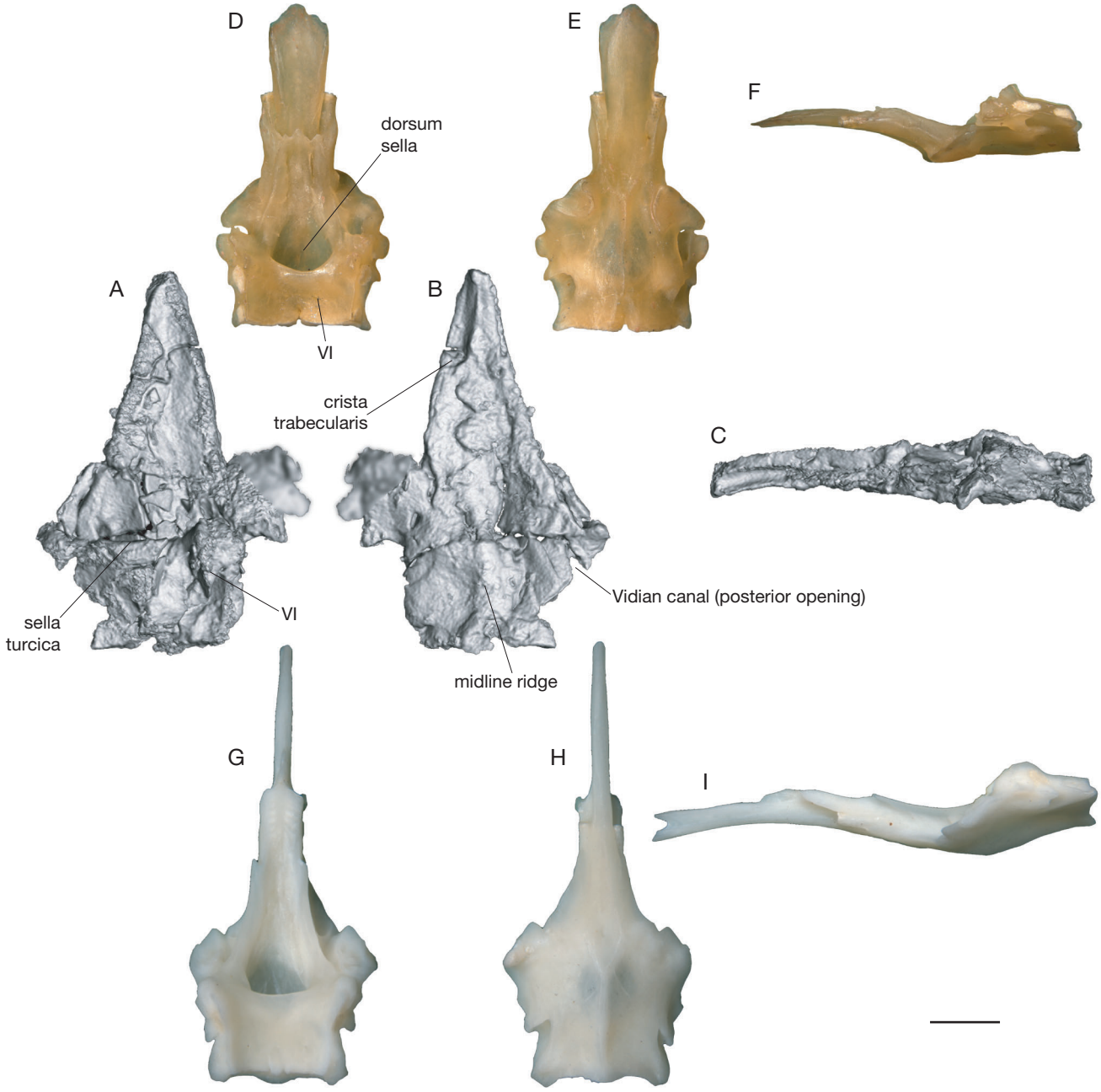

Fig. 5. — Parabasisphenoid: **A**-**C**, parabasisphenoid of HLMD-Me 9723, holotype of *Rageryx schmidi* n. gen., n. sp., in dorsal, ventral, and left lateral views, respectively. Portions of the parietal that articulated with the basisphenoid wings are probably artifactually associated here (blurred), but a more precise separation is not possible; **D**-**F**, parabasisphenoid of *Eryx johnii* BM 1930.5.8.31 in dorsal, ventral, and left lateral views, respectively; **G**-**I**, parabasisphenoid of *Lichanura trivirgata* CM 145332 in dorsal, ventral, and left lateral views, respectively. Scale bar: A-C, 1 mm; D-I, 2 mm.

of the facial nerve (VIIh) opens within the trigeminofacialis chamber, and well within the margins of the lateral opening of V3. Dorsally the prootic evinces an elongate groove for the reception of the supratemporal.

In ventral view the prootic exhibits an ophidiosphenoid foramen anteriorly (Fig. 6C), like in many boids but unlike in *Ungaliophis continentalis* Müller, 1880. There is an anteromedially trending groove that would have continued into the posterior opening of the Vidian canal on the basisphenoid. At the base of the groove is a relatively large foramen for the palatine ramus of cranial nerve VII, and the dorsolateral margin of the groove is expanded as a shelf that obscures said foramen in lateral view. A groove as such has a capricious phylogenetic distribution. *Lichanura trivirgata* (Fig. 6I) and *Charina bottae*, but not Ungaliophiinae or *Eryx* (Fig. 6F), share with HLMD-Me 9723 the shelf that obscures the foramen for the palatine branch of the facial nerve (VIIp). The ventral edge of the prootic in HLMD-Me 9723 is wedge-shaped, fitting into the broad notch between the parabasisphenoid anteriorly and basioccipital posteriorly.

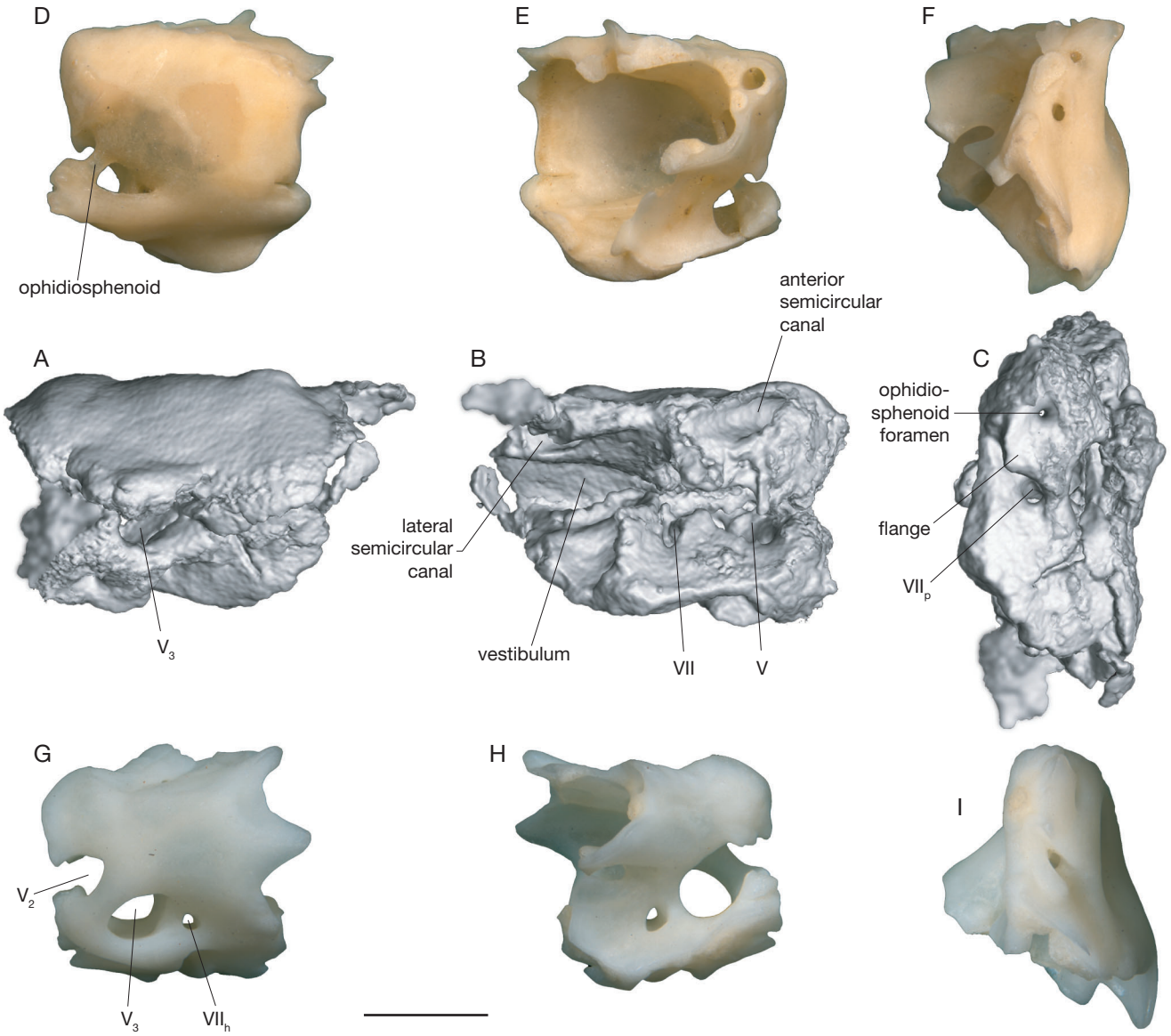

FIG. 6. — Prootic: **A**-**C**, left prootic of HLMD-Me 9723, holotype of *Rageryx schmidi* n. gen., n. sp., in lateral, medial, and ventral views, respectively. A small portion of the parietal is probably artifactually associated here (blurred), but a more precise separation is not possible; **D**-**F**, left prootic of *Eryx johnii* BM 1930.5.8.31 in lateral, medial, and ventral views, respectively; **G**-**I**, left prootic of *Lichanura trivirgata* CM 145332 in lateral, medial, and ventral views, respectively. Scale bar: A-C, 1 mm; D-I, 2 mm.

In medial view two foramina, a larger anterior opening for cranial nerve V and a smaller posterior opening for cranial nerve VII, pierce the cranial vault to enter the trigeminofacialis chamber (Fig. 6B). The impression of the vestibulum and parts of the relatively large anterior and lateral semicircular canals can be seen. In contrast to *Eryx*, in particular (Fig. 6E), the vestibulum is relatively small. The anterior semicircular canal extends to the anterior margin of the bone and well away from the vestibulum.

Supraoccipital

The supraoccipital achieves significant exposure between the parietal and otoccipitals (Fig. 1B), comparable to *Loxocemus bicolor*, *Lichanura trivirgata* and *Charina bottae*, but unlike in *Eryx* (Cundall & Irish 2008). Anteriorly on the midline a small prong projects into a corresponding notch in the posterior margin of the parietal.

*Otooccipital (*sensu *Maisano & Rieppel 2007)*

This paired element is poorly exposed, and segmentation was deemed too subjective due to crushing. The dorsal flanges of the otooccipitals meet broadly on the midline behind the supraoccipital, thereby forming the dorsal margin of the foramen magnum as in other snakes.

Supratemporal (Appendix 1: Fig. S8)

The supratemporal is an elongate element, weakly convex ventrally and weakly concave dorsally, with rounded anterior and posterior ends (Fig. 1B). Dorsolaterally at the posterior end is a facet for the quadrate articulation. Just

anterior to this facet the bone has dorsal bulge that is mirrored by a concavity on the ventral surface. The free end of the supratemporal is very short, extending only slightly beyond the otooccipital.

Quadrate (Appendix 1: Fig. S9)
The quadrate consists of a transversely oriented ventral condyle that articulates with the mandible and an oblique, triangular dorsal portion that contacts the supratemporal (Fig. 1B). The overall triangular shape is comparable to that in Ungaliophiinae, Charininae and *Eryx*. The ratio of the width of the cephalic condyle of the quadrate to the bone's height is 0.55, comparable to Ungaliophiinae (*c.* 0.53 in *Exiliboa placata* Bogert, 1968, 0.55 in *Ungaliophis continentalis*) and *Lichanura trivirgata* (0.49) but unlike Boinae (0.29 in *Candoia carinata*, 0.33 in *Boa imperator* Daudin, 1803), *Charina bottae* (0.43), and *Eryx* (0.44 in *Er. tataricus*). The quadrate is therefore relatively short and broad. A thick suprastapedial process (not "extrastapedial process" as in Smith 2013) projects ventrally from the medial edge of the bone; as it curves slightly anteriorly, it is hidden in lateral aspect. There is a prominent foramen in the dorsal portion of the bone on both right and left sides, which therefore cannot be attributed to an artifact; a comparable feature was not observed in any extant boid (although a small foramen in roughly this position is found in *Exiliboa placata*). Another, smaller foramen pierces the anterior surface of the shaft just above the ventral condyle; such a foramen is present in numerous boids.

Septomaxilla
The dorsolateral process of the left element is preserved, but the posterior spine is broken (Fig. 1B). Little more can be discerned.

Vomer
The vomers are presumably present but not clearly identifiable due to crushing.

Palatine
At least the right palatine is almost certainly present, but it cannot be recognized clearly due to crushing.

Pterygoid (Fig. 7; Appendix 1: Figs S10, S11)
The pterygoid is best represented by the left element (anteriorly) and the right element (posteriorly). The anterior portion (that portion anterior to the ectopterygoid articulation) is long, comparable to the posterior portion (Fig. 7A, B). In this it is similar to *Charina bottae* and relatively longer than in *Lichanura trivirgata* (Fig. 7G, H), *Eryx conicus* and *Boa imperator*; in other examined *Eryx* the anterior portion is much shorter than the posterior portion (Fig. 7E, F). The ectopterygoid process evinces a deep, roughly circular ectopterygoid facet, but the ectopterygoid process is not prominent (Fig. 7A); it is comparable to Boinae and some *Eryx* like *Er. johnii* (Fig. 7A) rather than *Lichanura trivirgata* (Fig. 7G) and *Charina bottae*.

The anterior portion is toothed ventrally (Fig. 7B). A single row of at least seven – and, if the tooth row continued as far posteriorly as the ectopterygoid articulation, as in other erycines, at least twelve – loci. The posterior portion (quadrate ramus) tapers continuously toward the sharp tip. As in *Li. trivirgata* (Fig. 7G) and *Ch. bottae*, it evinces a longitudinal dorsal groove (Fig. 7C). There is a medially or dorsally open groove in all examined *Eryx* (Fig. 7E), Boinae and Ungaliophiinae in the distal part of the quadrate ramus, but it represents a different surface of the bone; namely the medial edge crosses over dorsally to become the lateral edge of the bone, so the groove actually represents the ventral surface of the bone in Charininae.

Ectopterygoid (Fig. 8; Appendix 1: Fig. S12)
The left ectopterygoid (Fig. 8A, B) is the better preserved one; the portion after the anterior break is easily back-rotated. The bone as a whole is nearly straight, unlike the slightly curved element in many extant erycines (Fig. 8C-F) and *Xenopeltis unicolor* and the more strongly curved element of other constrictors. It shares with erycines the apomorphic absence of a sharp lateral corner. The bone grows in width anteriorly, like in most erycines, and evinces an articulation facet for the maxilla ventrally (Fig. 8B); the anterior end is simple and rounded. The bone becomes more robust posteriorly and has an expanded, posteromedially directed facet for the pterygoid; this facet is better developed than in most erycines, particularly *Lichanura trivirgata* (Fig. 8E, F).

Dentary (Fig. 9; Appendix 1: Fig. S13)
The dentary curves distinctly medially at its anterior end (Fig. 9A, B), more broadly so than in any examined boids (Fig. 9E, H) except Ungaliophiinae. The anterior end of the bone is also slightly downturned (Fig. 9C, D), like in Ungaliophiinae but unlike extant erycines (Fig. 9F, G, I, J). There is a single, large, anteriorly opening mental foramen at about the level of the 6th tooth. The subdental shelf is deep. The Meckelian groove is fully open and runs along the ventromedial edge of the bone. The connections with the postdentary bones are damaged and cannot be made out clearly. There is a deep notch for the compound bone, and the posterodorsal dentigerous and posteroventral processes appear to be roughly the same length, as in extant erycines (Fig. 9F, I) and *Ungaliophis continentalis* (but not *Exiliboa placata*).

Splenial
The splenial cannot clearly be made out.

Coronoid (Appendix 1: Fig. S14)
A coronoid is closely associated with the medial surface of the anterior end of the compound bone (Fig. 10D). It is short and weakly arched, with a concave anterodorsal and convex posteroventral margin. A strong, anteriorly trending process is lacking, so the bone lacks the L-shape seen in *Boa imperator* and all *Eryx* where the bone could be examined (i.e., *Er. colubrinus, Er. conicus, Er. jaculus, Er. jayakari, Er. muel-*

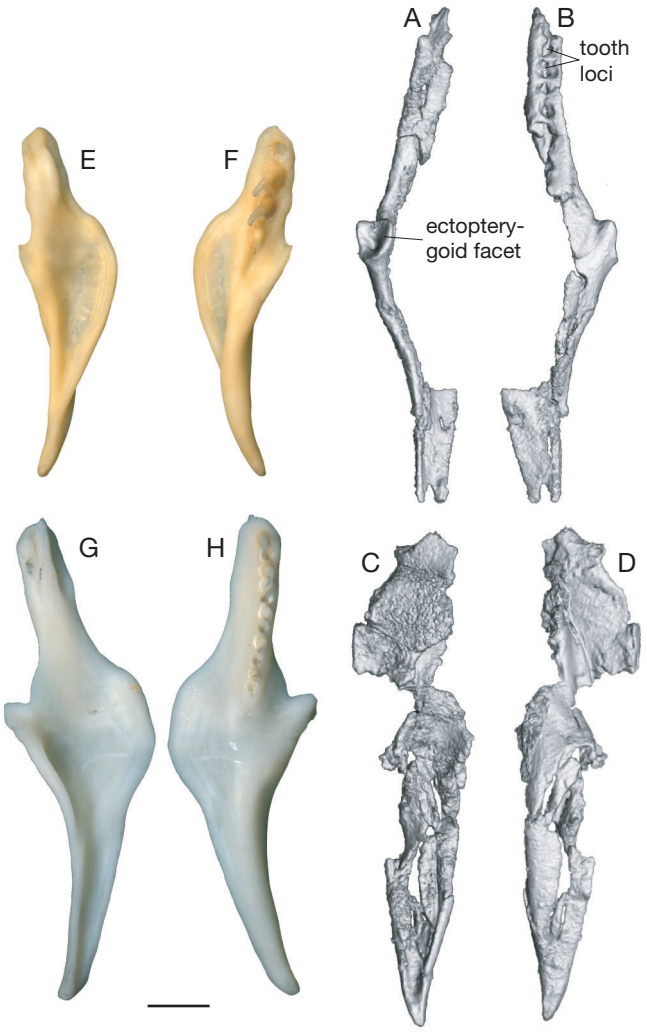

Fig. 7. — Pterygoid: **A**, **B**, left pterygoid of HLMD-Me 9723, holotype of *Rageryx schmidi* n. gen., n. sp., in dorsal and ventral views, respectively; **C**, **D**, right pterygoid of HLMD-Me 9723, holotype of *Rageryx schmidi* n. gen., n. sp., in dorsal and ventral views, respectively; **E**, **F**, left pterygoid of *Eryx johnii* BM 1930.5.8.31 in dorsal and ventral views, respectively; **G**, **H**, left pterygoid of *Lichanura trivirgata* CM 145332 in dorsal and ventral views, respectively. Scale bar: A-D, 1 mm; E-H, 2 mm.

leri) as well as fossil taxa *Messelophis variatus* Baszio, 2004 and *Rieppelophis ermannorum* (Schaal & Baszio, 2004) from Messel (Scanferla *et al.* 2016). Yet, it is not so highly reduced as in *Lichanura trivirgata*, much less completely absent, as in *Charina bottae* (Kluge 1993) and Ungaliophiinae.

Angular

The angular cannot clearly be made out.

Compound bone (Fig. 10; Appendix 1: Fig. S14)

Part of the large surangular process can be distinguished anteriorly, including a medially directed ridge that inserted beneath the dentary tooth row (Fig. 10D). Behind the dentary articulation, there is a fine groove roughly between the surangular and prearticular portions of the bone; however, this groove continues posteriorly, longitudinally transects the glenoid fossa (Fig. 10A), and extends ventrally through the compound bone only on the posterior portion, so it must be an artifact rather than an indication of incomplete fusion of surangular and prearticular.

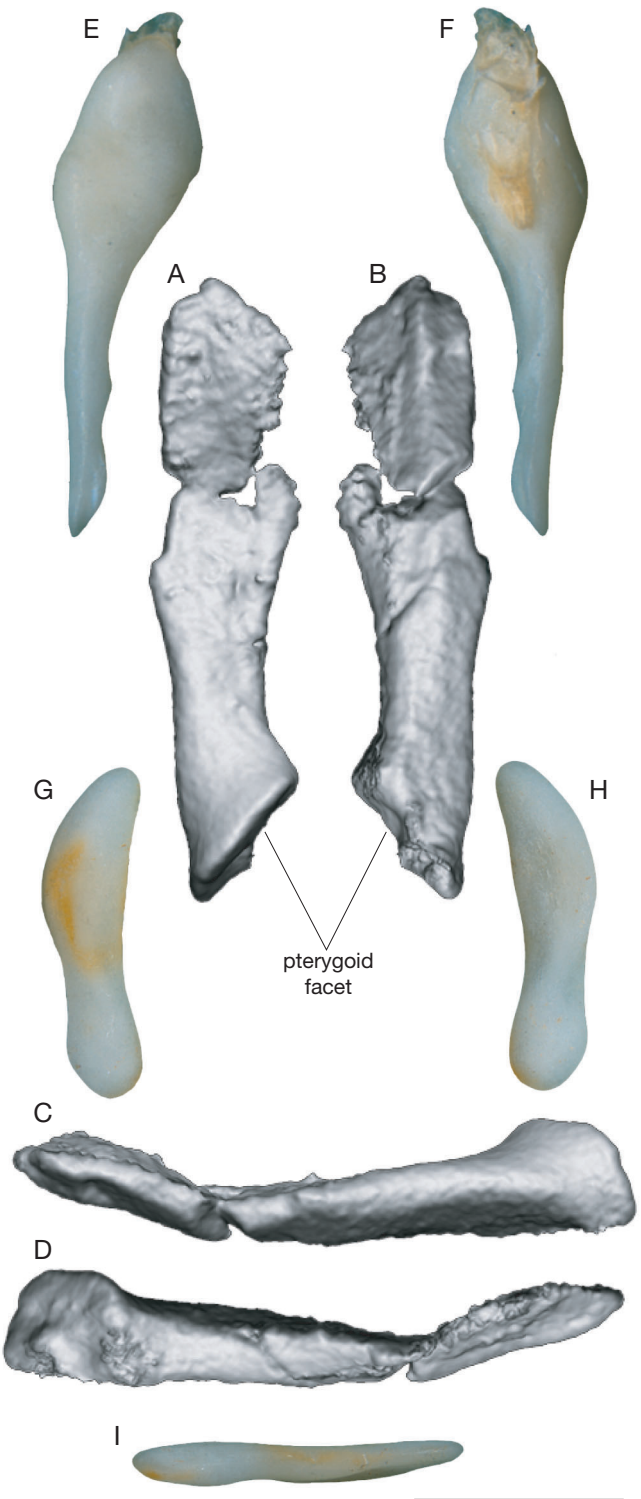

Fig. 8. — Ectopterygoid: **A-D**, left ectopterygoid of HLMD-Me 9723, holotype of *Rageryx schmidi* n. gen., n. sp., in dorsal, ventral, lateral, and medial views, respectively; **E**, **F**, right ectopterygoid (mirrored) of *Eryx jayakari* BM 1909.10.15.8 in dorsal and ventral views, respectively; **G-I**, left ectopterygoid of *Lichanura trivirgata* CM 145332 in dorsal, ventral, and medial views, respectively. Scale bar: A-D, 1 mm; E-I, 2 mm.

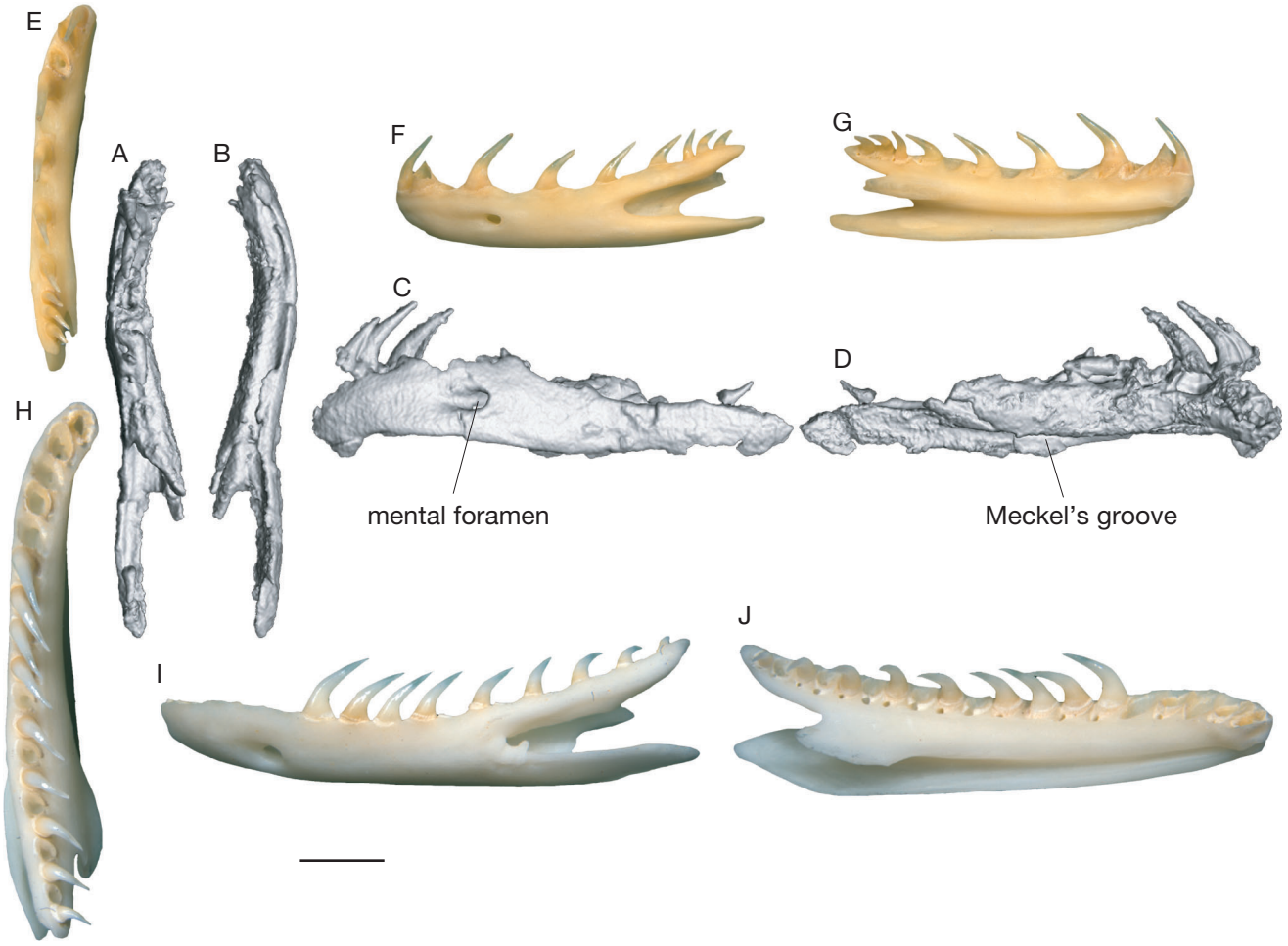

Fig. 9. — Dentary: **A**-**D**, left dentary of HLMD-Me 9723, holotype of *Rageryx schmidi* n. gen., n. sp., in dorsal, ventral, lateral, and medial views, respectively; **E**-**G**, left dentary of *Eryx johnii* BM 1930.5.8.31 in dorsal, lateral, and medial views, respectively; **H**-**J**, left dentary of *Lichanura trivirgata* CM 145332 in dorsal, lateral, and medial views, respectively. Scale bar: A-D, 1 mm; E-J, 2 mm.

The lateral surangular crest rises straight and gradually toward the coronoid eminence (Fig. 10C, D); its dorsal extent is approximately equal to that of the coronoid itself, so that both bones contribute to the coronoid eminence (Fig. 10D). The anterior margin of the compound bone contribution to this eminence decays more gradually, like in *Eryx* (Fig. 10G, H) and *Candoia carinata* and unlike in *Lichanura trivirgata* (Fig. 10K, L), *Charina bottae*, *Boa imperator* and Ungaliophiinae. The dorsal extent of the coronoid eminence is similar to that in other erycines. The medial, prearticular crest is low and nearly straight (Fig. 10D). It is nowhere visible behind the surangular crest in lateral aspect, unlike in examined boids except *Ca. carinata* and the erycines *Er. colubrinus, Er. jayakari, Er. muelleri* and *Ch. bottae*. Between them is the deep adductor fossa (Fig. 10A). Just below the coronoid eminence on the lateral surface is the anterior surangular foramen (Fig. 10C). Near the ventral margin on the lateral surface is a longitudinal ridge, also seen in some extant erycines. The retroarticular process is slightly longer than in most extant erycines and Ungaliophiinae.

Dentition

It is not the teeth at the very front of the maxilla that are the longest but rather those in the middle of the anterior half (Fig. 2B). Moving from front to back, that is, tooth length increases at first slightly before decreasing for most of the length of the jaw.

The maxillary tooth count can only be given approximately due to damage to both elements. On the left side, there is a toothless gap in the middle (Fig. 2B); based on the average length of the three preceding and three succeeding tooth bases, we estimate that this gap corresponds to approximately five teeth. There are four teeth at the front, and alveoli for seven teeth behind, for a total tooth count of *c.* 16. This value is higher than in most erycines, except for *Lichanura trivirgata* (Kluge 1993), but is lower than in most other constrictors (Underwood 1976). The count is comparable to that seen in Ungaliophiinae.

The dentary teeth appear to be broadly comparable to those of the maxilla, with longer teeth anteriorly than posteriorly (Fig. 9C, D). However, a tooth count cannot be given due to damage.

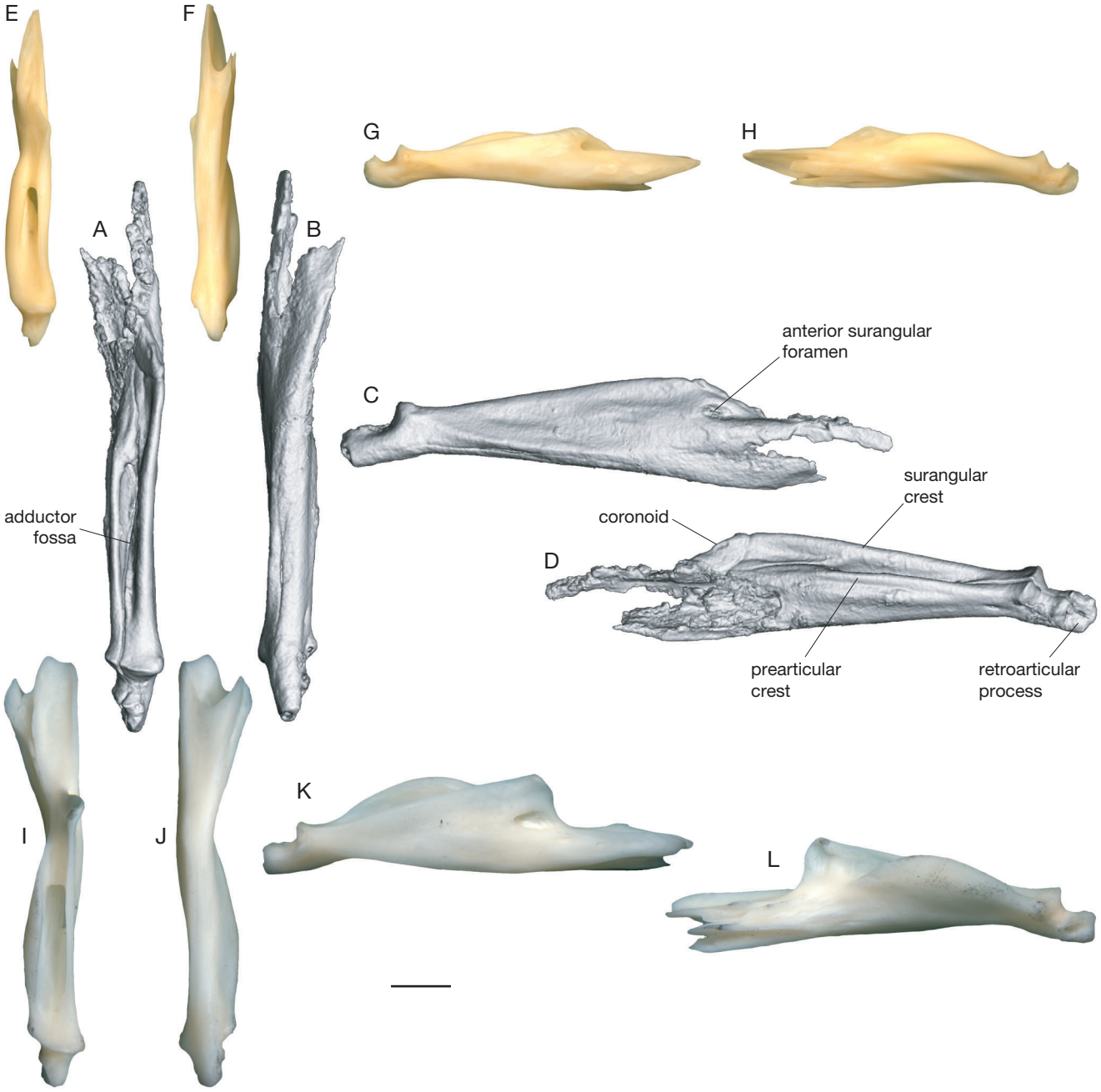

FIG. 10. — Compound bone: **A-D**, left compound bone of HLMD-Me 9723, holotype of *Rageryx schmidi* n. gen., n. sp., in dorsal, ventral, lateral, and medial views, respectively; **E-H**, left compound bone of *Eryx johnii* BM 1930.5.8.31 in dorsal, ventral, lateral, and medial views, respectively; **I-L**, left compound bone of *Lichanura trivirgata* CM 145332 in dorsal, ventral, lateral, and medial views, respectively. Scale bar: A-D, 1 mm; E-L, 2 mm.

Postcranial skeleton (Figs. 11; Appendix 1: S15-S17)

Hind limb rudiments are lacking, so the postcranial skeleton comprises only vertebrae and ribs. With measurements of the average length of four preceding and four succeeding vertebrae that bracket the gaps, and an estimate of the trend of the vertebral column, sometimes supported by the presered ribs, we arrive at an estimate of 258 total vertebrae, of which 220 are precloacal and 38 are cloacal or postcloacal (Appendix 1: Fig. S17). Accordingly 14.7% of the individual vertebrae are caudals (cloacals or postcloacals), comparable to the proportion observed in the three extant ungaliophiine species (14-17%) and that estimated for fossil *Calamagras weigeli* from the late Eocene of North America (14%, with 95% confidence interval 8-22%; Smith 2013). *Lichanura trivirgata* SMF-PH 21 has 236 precloacal vertebrae and 45 caudals (plus tail tip; see below), yielding 16%. A tail tip, apparently composed in part of fused vertebrae (Smith 2013), is present in HLMD-Me 9723 as well.

Anterior trunk vertebrae are defined as those vertebrae after the skull possessing a distinct hypapophysis. It forms a posteroventrally directed spine (Appendix 1: Fig. S15), with the fore margin becoming straighter and more horizontal on

more posterior vertebrae. Anterior trunk vertebrae number 52-68 (the boundary between anterior and mid-trunk vertebrae falls in the first gap of approximately 16 missing vertebrae). Thus, the fraction of the trunk vertebrae belonging to the anterior trunk is 0.24-0.31, compared with 0.18 (95% confidence interval 0.11-0.29) in fossil *Calamagras weigeli*, 0.19 in *Charina bottae*, 0.25-0.28 in *Ungaliophis* and 0.35 in *Exiliboa placata* (Smith 2013). The neural arches ("tecta" of Jandzík & Bartík 2004) of the atlas are broad (i.e., anteroposteriorly long). The axis and succeeding three vertebrae have rodlike and strongly posteriorly inclined neural arches that project beyond the posterior margin of the neural arch. On the seventh precloacal vertebra the neural spine bears an anterior expansion, which rapidly grows in strength on more posterior vertebrae. By the 10th the neural spine is strong and more dorsally directed, so that it no longer (or just barely) projects beyond the posterior margin of the neural arch. On these more anterior vertebrae the postzygapophyses are angular, suggesting small or narrow zygapophyseal articulations; additionally, they are very (anteroposteriorly) short. On more posterior anterior trunk vertebrae the neural spine appears to become recumbent again, overhanging the notch in the posterior margin of the neural arch. The neural spine becomes less prominent and is anteroposteriorly short, as judged by the finished cap at its distal end, although it is prolonged by a thin, sharp ridge of bone with an oblique anterior margin that runs as far as the base of the zygosphene. A low, oval zygantral mound that creates space in the zygantrum for accomodation of the zygosphene (Hecht *in* McGrew *et al.* 1959) is present on all anterior trunk vertebrae. Vertebral length increases through the preserved portion of the anterior trunk vertebrae.

The mid-trunk vertebral series, as far as it is preserved, commences after the first gap and continues past the second gap (*c.* 14 vertebrae) and third gap (*c.* 4 vertebrae). Almost all of the neural spines are broken, but they appear to have been low and short, to judge by the broken edge. The zygantral mounds become more prominent, and on the anterior mid-trunk vertebrae they occur in conjunction with a flaring of the posterior margin of the neural arch beyond the level defined by the postzygapophyses. This flaring disappears by about the middle of the vertebral column; thereafter, the posterior margin of the neural arch is transverse except for the triangular notch on the midline. Vertebral length reaches a maximum in the middle of the mid-trunk vertebrae. A mid-trunk vertebra was not segmented, as a CT scan is not available.

An exact boundary between the mid- and posterior (Appendix 1: Fig. S16) trunk vertebrae cannot be drawn, but vertebral length gradually decreases toward the posterior end of the precloacal vertebral column. The vertebrae also appear to become relatively shorter. The notch on the posterior margin of the neural arch becomes broader, and on the posterior-most posterior trunk vertebrae it is so broad that the transversality of the margin is obliterated and the postzygapophyses are once again angular. The zygantral mound disappears. The neural spine, where preserved, is very low but slightly longer. The neural arch is also more vaulted than in *Lichanura trivirgata* (Fig. 11A, posterior view) or *Eryx*. The anterior end of the zygosphene on a segmented posterior trunk vertebra appears to have a bulge (Fig. 11B, dorsal view), giving it a crenate shape (Auffenberg 1963).

The subcentral (lymphatic) grooves are very prominent on posterior trunk vertebrae, forming in the more posterior part of the series a slightly projecting keel or hypapophysis, which projects more strongly than in *Lichanura trivirgata* (Fig. 11A, lateral view), where it is ventrally flattened. However, the lateral expansions of the ventral keel seen in *Li. trivirgata* (Fig. 11A, ventral view) are absent. Prezygapophyseal accessory processes appear to be completely absent in HLMD-Me 9723 (Fig. 11B, ventral view), unlike the prominent processes in *Li. trivirgata* (Fig. 11A, dorsal view) and some *Eryx*.

Caudal vertebrae comprise cloacal and postcloacal vertebrae. At least two cloacal vertebrae were present; they are overlapped by the tail tip (Fig. 1D) and visible only through the epoxy plate and in the CT scan (Fig. 1E). They are identified by the fused, bifurcated, anteroventrally directed lymphapophyses, of which the dorsal spine appears to be the longer one (left side of first cloacal, broken on right).

The postcloacal vertebrae, lacking bifurcated lymphapophyses, are relatively short. However, the neural spine is relatively longer and mediolaterally thicker (Fig. 11C-E, dorsal and anterior views). Strictly speaking, it evinces no bifurcation anywhere, unlike in *Charina bottae*, *Lichanura trivirgata* (Fig. 11F) or *Eryx* spp., where the spine strongly expands in width distally and the tip presents a deep dorsal, midline groove. However, starting near mid-tail its anterior end is drawn out into a pair of short spines. A short zygosphene appears to be present on postcloacal vertebrae much closer to the tip than in *Lichanura trivirgata* (Fig. 11F, dorsal view) or *Eryx* spp.

A distinctive feature of the postcloacals is the height of the posterior margin of the neural arch. Even in the middle of the tail the neural arch is quite vaulted, and a flat, vertical posterior surface arises. The height of this surface diminishes distally in the tail. Such a surface is not observed in *Lichanura trivirgata*, but in some *Eryx* spp. a similar surface is present on anterior caudals.

The cotyle and condyle are small and round (Fig. 11D, anterior and posterior views). Paracotylar foramina appear to be present on the distalmost segmented caudal vertebra (Fig. 11E), but they are apparently absent anteriorly in the tail and on the segmented posterior trunk vertebra; it is possible that their apparent presence distally in the tail is an artifact (but see Zerova 1989; Georgalis 2019).

The dimensions of distal postcloacal vertebrae – short and tall – are comparable to those in extant erycines (Fig. 11F, lateral view). Moreover, at least some supernumerary vertebral processes are present on all preserved postcloacal vertebrae (Fig. 1D, E). We follow the terminology of Szyndlar (1994) in describing them. Pterapophyses are present as distinct bumps already on the first postcloacal preserved after the gap of *c.* 11 vertebrae; they grow rapidly in prominence dis-

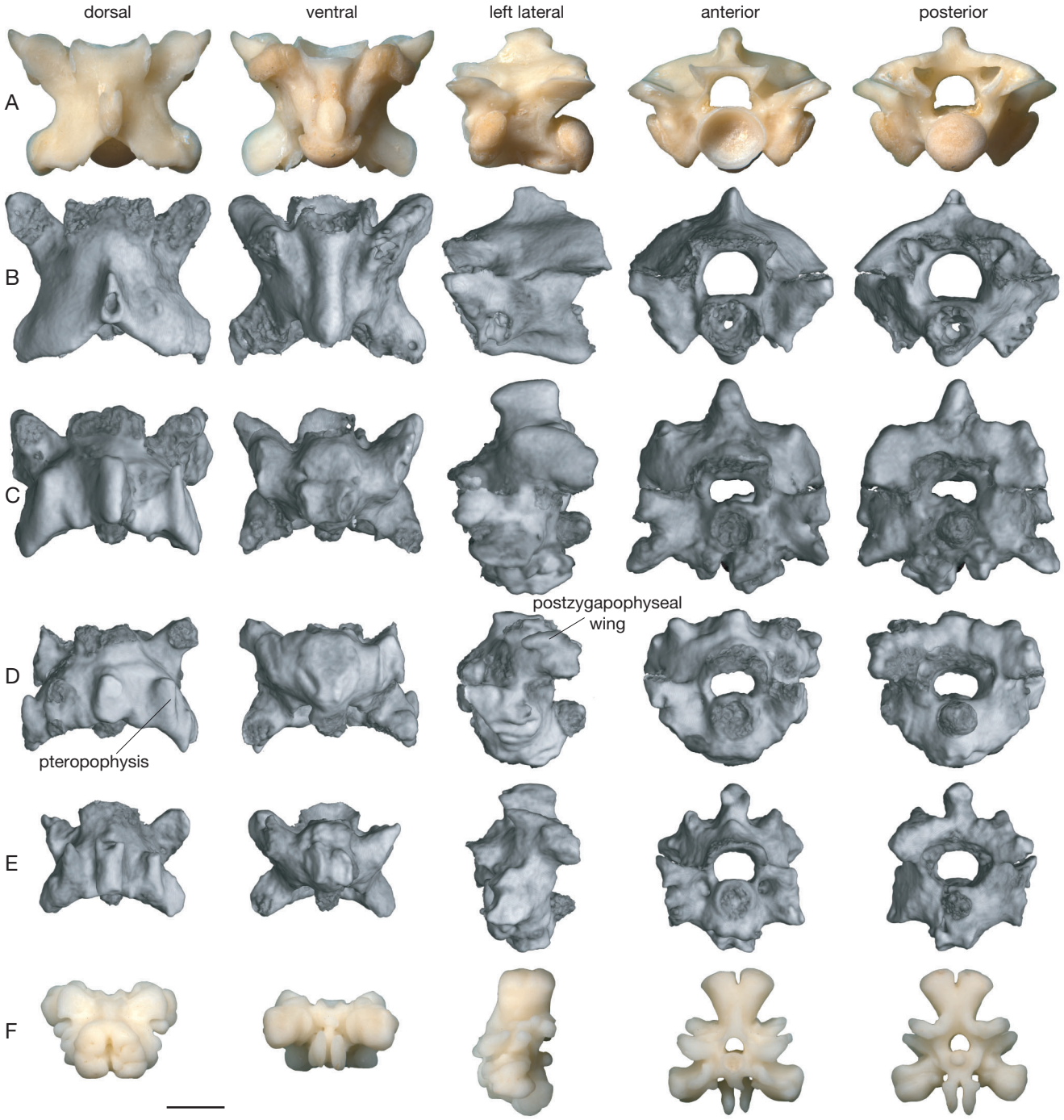

FIG. 11. — Vertebrae: **A**, posterior trunk vertebra (precloacal vertebra number 200) of *Lichanura trivirgata* SMF-PH 21; **B**, posterior trunk vertebra of HLMD-Me 9723, holotype of *Rageryx schmidi* n. gen., n. sp.; **C**-**E**, anterior, middle and distal caudal vertebrae of HLMD-Me 9723, holotype of *Rageryx schmidi* n. gen., n. sp.; **F**, distal caudal vertebra of *Lichanura trivirgata* CM 145332. Views: dorsal, ventral, left lateral, anterior, posterior. Scale bar: A, F, 2 mm; B-E, 1 mm.

tally in the tail, forming long, anteroposterior ridges with strong, anteriorly projecting spines (Fig. 11C-E). Curiously, similar spines are also present in *Pterygoboa* Holman, 1976 from the North American late Oligocene and Miocene (e.g., Holman 2000; Mead & Schubert 2013). Postzygapophyseal wings and posterior extensions of the prezygapophyses are not present anteriorly but become distinct by about the 16th caudal vertebra (after the gap); they never become prominent. Pleurapophyses were presumably present on all postcloacal vertebrae, but they are everywhere preserved; posteriorly in the tail they have a knoblike appearance distally, but a distinct posterior extension of the pleurapophyses appears to be absent. In addition to these main, named supernumerary processes, the distal-most caudal vertebrae in *Charina bottae* and *Eryx* spp. exhibit fine-scale elaborations of small, generally anteroposteriorly arranged ridges (Szyndlar 1994: fig. 2). Such elaborations are present on the distal-most caudals of HLMD-Me 9723 as well (Fig. 1D).

Hemapophyses are apparently present on all preserved postcloacal vertebrae (Fig. 11C-E, ventral view), but they are often broken. Thus, their length cannot be ascertained, nor is it known whether "tubercular prominences" of the hemapophyses (Sood 1941) were present.

The ribs are for the most part broadly rounded (Fig. 1A). In some cases the ribs appear to evince distinct bends, but because these appear sporadically and are bounded front and back by ribs of normal curvature, we ascribe the bends to plastic deformation. The ribs suggested a broadly rounded body, or at least one that was not markedly compressed or depressed.

Phylogenetic relations (see Appendix 2)

Phylogenetic analysis using MP produced 126 equally most-parsimonious trees, the strict consensus of which is shown in Fig. 12A. The relationships of basal alethinophidians are fully unresolved. *Xenopeltis unicolor* and *Loxocemus bicolor* are successive outgroups to a clade comprising the Cretaceous marine snakes and Henophidia sensu Gauthier *et al.* (2012), and a sister-group relationship between *Lo. bicolor* and fossil *Ogmophis compactus* (Smith 2013) is confirmed (although bootstrap support is low). Ungaliophiinae forms a clade with *Calamagras weigeli*, also confirming the conclusion of Smith (2013); as above, bootstrap support is low, and whether *Cal. weigeli* is inside the crown is unresolved (Smith 2013; Fig. 12A). Booidea sensu Pyron *et al.* (2014) is not monophyletic; instead, as is typical in phylogenetic analyses of morphology (Lee & Scanlon 2002; Gauthier *et al.* 2012; Hsiang *et al.* 2015), the large boas, or Boidae sensu Pyron *et al.* (2014), and pythons, or Pythonidae sensu Reynolds *et al.* (2014), cluster together. Unlike in molecular analyses, erycines including *Eryx* and Charininae form a clade that also includes *Rageryx schmidi* n. gen., n. sp., which forms the sister-taxon to Charininae. Enforcing a molecular constraint on the tree topology did not influence the placement of any of these three fossil taxa.

Synapomorphies supporting the clade *Rageryx schmidi* n. gen., n. sp. and Charininae are as follows: ventral extent of postorbital reduced, quadrate ramus of pterygoid horizontally bladelike with longitudinal dorsal groove, exit foramen for hyomandibular branch of cranial nerve VII obscured in lateral view by projecting flange of prootic, and coronoid reduced. Autapomorphies of *Rageryx schmidi* n. gen., n. sp. according to this analysis are generally reversals, particularly of synapomorphies common to the broader group of erycines, viz. loss of protruding premaxilla and gain of zygosphene-zygantral articulations distally in the tail. The exception is the presence of a posteromedial flange for the ectopterygoid. Given the strong molecular evidence of erycine polyphyly, the putative reversals should be viewed with caution.

Similar relations for the booid fossil taxa are inferred using standard BI (Fig. 12B). The posterior probability (PP) for the clade *Rageryx schmidi* n. gen., n. sp. + Charininae is 0.98. *Calamagras weigeli* comes out in the crown of Ungaliophiinae, albeit with low support (PP = 0.59). *Ogmophis compactus* is the sister-taxon to *Loxocemus bicolor*, similarly with low support (PP = 0.56).

Insofar as it incorporates the age of fossil taxa, BI using the fossilized birth-death model gave results that differed from those of the MP analysis in expected ways. Without topological constraints, *Ogmophis compactus* (at *c.* 35 Ma) falls to the stem of a clade *Loxocemus* + *Xenopeltis*. *Calamagras weigeli* (at *c.* 48 Ma) falls to the stem of Ungaliophiinae; and *Rageryx schmidi* n. gen., n. sp. (also at *c.* 48 Ma) falls to the stem of Charininae. Support for these relationships is low. When minimum molecular topological constraints are enforced, *Rageryx schmidi* n. gen., n. sp. is strongly supported (PP > 0.99) as a stem representative of Charininae (PP > 0.99), and *Cal. weigeli* strongly supported (PP > 0.99) as a stem representative of Ungaliophiinae (PP > 0.99). The position of *Ogmophis compactus* with respect to *Xenopeltis*, *Loxocemus*, and Pythonidae, however, is poorly resolved.

Thus a sister-group relationship between *Rageryx schmidi* n. gen., n. sp. and crown Charininae is well supported, making the former the oldest confirmed fossil erycine. Because no new data were adduced concerning *Messelophis variatus* and *Rieppelophis ermannorum*, it is not surprising that their relationships to other booids are unresolved, as in Scanferla *et al.* (2016).

DISCUSSION

Paleoecology

Rarely in extant snakes – specifically, in all extant erycines, the basal uropeltid *Melanophidium wynaudense* (Beddome, 1863) (Rieppel & Zaher 2002: fig. 2A), and the primitive constrictor *Loxocemus bicolor* as well as the pythonid *Aspidites melanocephalus* (Krefft, 1864), among examined snakes – the premaxilla is protruded far forward of the arch defined by the maxillae. (Note that this protrusion of the premaxilla is much stronger than the slight protrusion documented by Longrich *et al.* [2012: char 162] in Macrostomata more generally.) This feature might be seen as an intermediate stage in the evolution of a wedge-shaped digging snout and countersunk jaws, and such further developments are seen in only a few of the taxa possessing the protruding premaxilla (e.g., *Eryx somalicus*, *Er. tataricus*, *Loxocemus bicolor*). Rieppel (1978a) pointed out that erycines (except *Lichanura*) display a transversely expanded premaxilla that supports the rostral shield, both thus assembling a broad horizontal digging edge. On the other hand, Frazzetta (1975) suggested that protecting the snout in case of miscalculated strikes that miss prey and hit other objects could also have a selective influence on the premaxilla. Regardless, a protruding wedge-shaped snout can safely be excluded for *Rageryx schmidi* n. gen., n. sp.

The snout in snakes is suspended from the remainder of the skull by a nasofrontal joint, which is absent in lizards (Rieppel 1978b). In a number of fossorial taxa, however, the joint has been greatly expanded by a thickening of the ventral portion of the medial and lateral frontal pillars and the formation of a transverse articulation for the medial nasal flanges. These taxa include erycines (Rieppel 1978a) as well as Uropeltidae (Olori & Bell 2012), *Anomochilus*

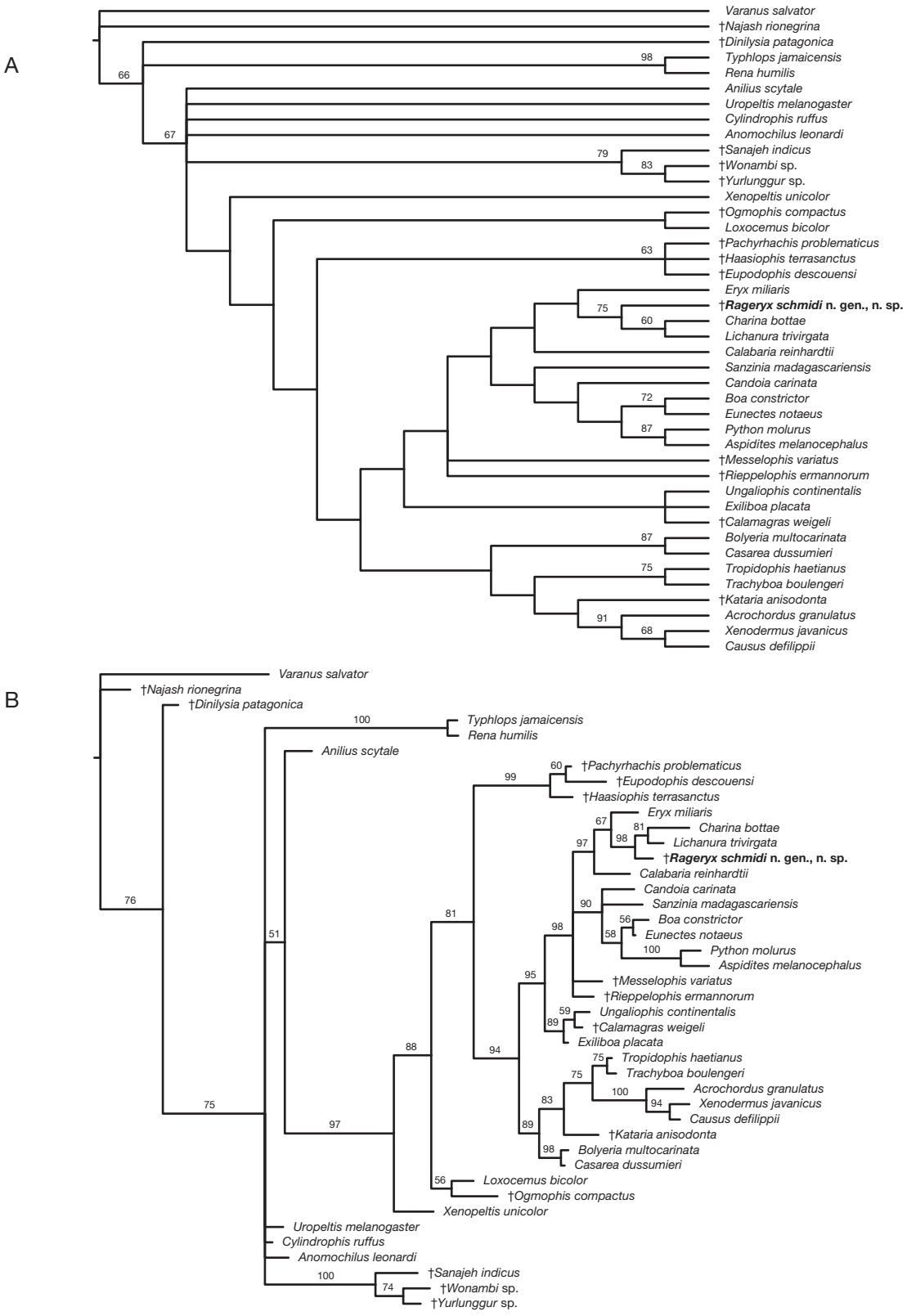

FIG. 12. — Phylogenetic relationships of *Rageryx schmidi* n. gen., n. sp.: **A**, strict consensus of 176 equally most-parsimonious trees; bootstrap percentages >50% are shown above branches; **B**, majority-rule consensus of 15 000 trees from standard Bayesian analysis. Posterior probabilities are shown above branches.

Smith, 1940, *Cylindrophis* Wagler, 1828 and, strangely, *Boa imperator* (pers. obs.). This configuration may reinforce or buttress the snout to permit digging while not hindering the swallowing of relatively large prey (Rieppel 1978a). These character states were interpreted as an adaptation for stabilizing the snout during head-first digging (Rieppel 1978a).

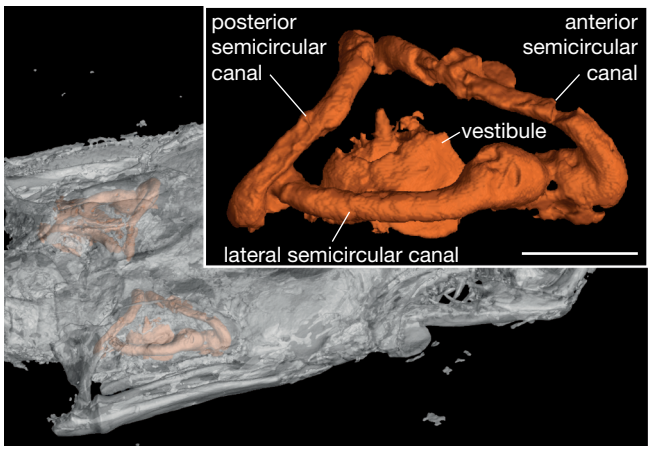

Fig. 13. — Inner ear of HLMD-Me 9723, holotype of *Rageryx schmidi* n. gen., n. sp. Semitransparent skull for orientation, showing location of left and right bony labyrinth, with inset showing enlarged right inner ear. Scale bar: 1 mm.

Notably, Rieppel (1978a) considered the nasofrontal joint of *Lichanura trivirgata* to be unspecialized for digging, while our comparisons suggest it is similar to *Charina bottae*. Regardless, while the ventral parts of the nasal and frontal are crushed in HLMD-Me 9723, we considered above that it was unlikely that such a robust buttress joint could have been present and not be distinguishable. The apparent absence of this joint in HLMD-Me 9723 argues against active fossoriality. Still, the large morphological diversity of extant forms that occupy different macrohabitats, as well as the realization that extant snakes can burrow with a fully kinetic snout (Deufel 2017) invites caution.

The inner ear of burrowing squamates also shows a consistent set of adaptations, which were recently explored (Yi & Norell 2015). These include a large and spherical vestibule (which, presumably containing a large saccular otolith, is more sensitive to low-frequency ground vibrations), a large foramen ovale (correlated with a large stapedial footplate), slender semicircular canals that are scarcely separated from the vestibule, and a vestibular lumen (osseous labyrinth) that is confluent with the lateral semicircular canal (the "open lumen" condition described by Olori 2010). Not all of these features could be evaluated in HLMD-Me 9723, but the vestibule appears to have dimensions like those of generalist squamates (Yi & Norell 2015), the anterior and lateral semicircular canals are well separated from the vestibule, and the semicircular canals are neither markedly expanded (as in some Scolecophidia) nor very slender (as in other squamate burrowers) (Yi & Norell 2015). Thus, the inner ear also evinces no particular adaptations for fossoriality (Fig. 13).

Remarkably, in spite of the lack of any exceptional adaptations for fossorial habits in the cranial skeleton (modifications of premaxilla, nasofrontal joint buttresses, bony labyrinth), the tail tip exhibits the modifications found to greater or lesser degree in all extant erycines (Bogert 1968; Szyndlar & Rage 2003; Smith 2013): the supernumerary processes. The function of these processes in extant erycines is poorly understood.

Three hypotheses have been proposed to explain the occurrence of the accessory processes in erycines. First, Hoffstetter & Gasc (1969: 297) suggested "the blunt tails of some species might be used as a lever in burrowing" (Greene 1973: 153). Second, Greene (1973) suggested that the modifications of caudal vertebrae were originally related to a defensive display function, enabling the tails to "withstand repeated attacks." He buttressed his argument with data on the prevalence of tail injuries in different species (especially *Eryx johnii* and *Charina bottae*), but noted that the modifications could also have been exapted (sensu Gould & Vrba 1982) for burrowing. Third, Hoyer (1974) suggested that injuries in *Ch. bottae* primarily result from warding off prey (specifically, the parents of altricial rodents); he supported his supposition with the observation that scarring incidence is greater in females (see also Hoyer & Stewart 2000), which are larger and may need more food, but did not conduct interspecies comparisons. Accordingly, the accessory processes reinforce the tail tip to withstand repeated attacks not from predators but from prey. Insofar as they may serve a selective purpose, the prominent modifications of erycines could be the result of convergence (Greene 1973). Insofar as it does not show evidence of fossoriality, the occurrence of the accessory processes in *Rageryx schmidi* n. gen., n. sp. is not consistent with the first hypothesis, and a defensive role, particularly a role in defensive display, may be entertained.

While erycines today are restricted to semiarid habitats and show a marked proclivity for burrowing, we are dealing here with a stem representative, so that these non-preserved aspects of fossil species cannot necessarily be attributed to *Rageryx schmidi* n. gen., n. sp. Moreover, whereas ecomorphological features that can be interpreted as adaptations for a particular lifestyle could be used to infer ecology, the reasons for the modifications of the caudal skeleton in erycines are not yet clear (see above). Therefore, we are not justified in inferring that the Messel erycine is indicative of particular climatic or edaphic conditions.

Comments on the Messel snake fauna

Gut contents have been reported from the Messel snake *Palaeopython fischeri* Schaal, 2004 (Greene 1983; Smith & Scanferla 2016). Also, an embryo was reported in the body of the Messel snake *Messelophis variatus* (Smith *et al.* 2018). While these discoveries contribute to knowledge of the ecology of these species, there is unfortunately no indication of either in HLMD-Me 9723. However, preserved jaw bones of *Rageryx schmidi* n. gen., n. sp. shed some light on its dietary preferences. A short free-ending process of supratemporal and the small quadrate length indicate a reduced relative gape size in *Rageryx* n. gen., even smaller than in extant erycines such as *Charina* and *Lichanura*. Macrostomatan snakes with small gape frequently consume small and/or elongated prey (Cundall & Greene 2000; Scanferla 2016; Moon *et al.* 2019), thus suggesting that *Rageryx schmidi* n. gen., n. sp. also consumed this kind of prey.

Remarkably, of the four booid snake species recognized up to now in Messel, three of them (*Messelophis variatus*, *Riep-*

pelophis ermannorum and *Rageryx schmidi* n. gen., n. sp.) are small-sized forms and displayed a small gape (Scanferla 2016; Smith & Scanferla 2016). A size-based taphonomic filter does not appear to be good explanation for this pattern, because the large booid, *Palaeopython fischeri*, is relatively abundant at Messel (Schaal 2004; the relations of this genus remain unclear: Georgalis & Scheyer 2019). A complete picture of the snake diversity in Messel is far from being achieved, yet the pattern invites a brief comment. The early-middle Eocene Messel snake fauna is the oldest known assemblage of macrostomatan snakes that is documented through nearly complete skeletons. Thus, the presence of a high proportion of minute species with a small gape suggest that such forms may have formed a large and underrecognized component of the early evolutionary radiation of booids, and the later restriction of small body size to a few lineages (Charinidae, *Eryx*) is a phenomenon driven by extinction.

Biogeography

The closest living relatives of *Rageryx schmidi* n. gen., n. sp. are in North America, and particularly if Ungaliophiinae and Charininae are sister-taxa, the origin of the lineage is to be sought there. If "*Calamagras*" *gallicus* pertains to the same lineage, then it can be traced back to the early Eocene. Numerous other North American squamate lineages documented from the early Eocene of North America (Smith 2009a; Smith & Gauthier 2013) entered Europe near the Paleocene-Eocene Thermal Maximum (e.g., Augé 2003; Smith 2009b; Rage 2012), and this observation applies to other groups of vertebrates as well (e.g., Georgalis & Joyce 2017). These squamate lineages, many of which are documented at Messel, comprise corytophanine and polychrotine iguanids, glyptosaurine and potentially anguine anguids, helodermatids, and potentially the acrodont iguanian *Tinosaurus* Marsh, 1872 (but see Smith *et al.* 2011) and booids (see Smith *et al.* 2018). Further immigrants shared by Europe and North America in the early Eocene are the varanid lineage *Saniwa* Leidy, 1870 and shinisaurs (Smith 2017), and at least one lineage, the ?lacertoid *Scincoideus* Folie, Sigé & Smith, 2005, crossed from Europe to North America (Smith 2011). Particularly if Charininae is proven to be present in the North American early Eocene (Head & Holroyd 2008), the occurrence of *Rageryx* n. gen. in Messel highlights the taxonomic similarity of Euro-American squamate assemblages at the height of the Eocene Climate Optimum, a phenomenon recognized in mammals and other vertebrates (e.g., Savage & Russell 1977; McKenna 1983; Mayr 2009; Rose 2012; Georgalis & Joyce 2017).

Acknowledgements

We thank N. Micklich and T. Wappler (HLMD) for the opportunity to study the new Messel species. S. Köster (SMF) digitally segmented the bones and assembled the figures in the text. R. Posch and R. Kunz (SMF) gave tips for VG Studio. T. Lehmann (SMF) kindly translated the title and abstract into French. Access to modern comparative material was provided by P. Campbell (BM), S. Rogers (CM), L. Costeur (MBS), and D. Vasilyan (then University of Tübingen). We are indebted to Z. Szyndlar and G. Georgalis for their constructive reviews and for pointing out overlooked literature. Finally, we are grateful for the hospitality, generosity and wisdom of the late Jean-Claude Rage, who was originally intended to be an author on this paper and to whom this paper is dedicated in respectful memory.

REFERENCES

Auffenberg W. 1963. — The fossil snakes of Florida. *Tulane Studies in Zoology* 10: 131-216. https://doi.org/10.5962/bhl.part.4641

Augé M. 2003. — Lacertilian faunal change across the Paleocene-Eocene boundary in Europe, *in* Wing S. L., Gingerich P. D., Schmitz B. & Thomas E. (eds), *Causes and Consequences of Globally Warm Climates in the Early Paleogene*. Geological Society of America, Boulder: 441-453. https://doi.org/10.1130/0-8137-2369-8.441

Bogert C. M. 1968. — A new genus and species of dwarf boa from southern Mexico. *American Museum Novitates* 2354: 1-38. http://hdl.handle.net/2246/2564

Caldwell M. W., Nydam R. L., Palci A. & Apesteguía S. 2015. — The oldest known snakes from the Middle Jurassic-Lower Cretaceous provide insights on snake evolution. *Nature Communications* 6: 5996. https://doi.org/10.1038/ncomms6996

Cignoni P., Callieri M., Corsini M., Dellepiane M., Ganovelli F. & Ranzuglia G. 2008. — MeshLab: an open-source mesh processing tool, *in* Scarano V., De Chiara R. & Erra U. (eds), Proceedings of the Eurographics Italian Chapter Conference, 2008. The Eurographics Association: 129-136.

Cope E. D. 1873. — Synopsis of new Vertebrata from the Tertiary of Colorado, obtained during the summer of 1873. *Annual Report of the United States Geological Survey of the Territories* 7: 3-19. https://doi.org/10.3133/70039707

Cope E. D. 1883. — The Vertebrata of the Tertiary Formations of the West (Report of the United States Geological Survey of the Territories, Vol. III). Government Printing Office, Washington, D.C., 1009 p., pls I-LXXV. https://doi.org/10.3133/70038954

Cundall D. & Greene H. W. 2000. — Feeding in snakes, *in* Schwenk K. (ed.), *Feeding: Form, Function and Evolution in Tetrapod Vertebrates*. Academic Press, San Diego: 293-333. https://doi.org/10.1016/B978-012632590-4/50010-1

Cundall D. & Irish F. J. 2008. — The snake skull, *in* Gans C., Gaunt A. S. & Adler K. (eds), *Biology of the Reptilia*. Vol. 20 (Morphology H). *The Skull of Lepidosauria*. Society for the Study of Amphibians and Reptiles, Ithaca, New York: 349-692.

Deufel A. 2017. — Burrowing with a kinetic snout in a snake (Elapidae: *Aspidelaps scutatus*). *Journal of Morphology* 278: 1706-1715. https://doi.org/10.1002/jmor.20743

Franzen J. L. 2005. — The implications of the numerical dating of the Messel fossil deposit (Eocene, Germany) for mammalian biochronology. *Annales de Paléontologie* 91: 329-335. https://doi.org/10.1016/j.annpal.2005.04.002

Frazzetta T. H. 1975. — Pattern and instability in the evolving premaxilla of boine snakes. *American Zoologist* 15: 469-481. https://doi.org/10.1093/icb/15.2.469

Gauthier J., Kearney M., Maisano J. A., Rieppel O. & Behlke A. 2012. — Assembling the squamate tree of life: Perspectives from the phenotype and the fossil record. *Bulletin of the Peabody Museum of Natural History* 53: 3-308. https://doi.org/10.3374/014.053.0101

GEORGALIS G. L. 2019. — Poor but classic: the squamate fauna from the late Miocene of Pikermi, near Athens, Greece. *Comptes Rendus Palevol* 18 (7): 801-815. https://doi.org/10.1016/j.crpv.2019.09.004

GEORGALIS G. L. & JOYCE W. G. 2017. — A review of the fossil record of Old World turtles of the clade *Pan-Trionychidae*. *Bulletin of the Peabody Museum of Natural History* 58: 115-208. https://doi.org/10.3374/014.058.0106

GEORGALIS G. L. & SCHEYER T. M. 2019. — A new species of *Palaeopython* (Serpentes) and other extinct squamates from the Eocene of Dielsdorf (Zurich, Switzerland). *Swiss Journal of Geosciences* 112: 383-417. https://doi.org/10.1007/s00015-019-00341-6

GOTH K. 1990. — Der Messeler Ölschiefer – ein Algenlaminit. *Courier Forschungsinstitut Senckenberg* 131: 1-141.

GOULD S. J. & VRBA E. 1982. — Exaptation – a missing term in the science of form. *Paleobiology* 8: 4-15. https://doi.org/10.1017/S0094837300004310

GRADSTEIN F. M., OGG J. G., SCHMITZ M. D. & OGG G. M. 2012. — The Geologic Time Scale 2012, Vol. 1-2. Elsevier, Amsterdam, 1144 p.

GRAY J. E. 1825. — A synopsis of the genera of Reptiles and Amphibia, with a description of some new species. *Annals of Philosophy (Series 2)* 10: 193-217. https://www.biodiversitylibrary.org/page/2531387

GREENE H. W. 1973. — Defensive tail display by snakes and amphisbaenians. *Journal of Herpetology* 7: 143-161. https://doi.org/10.2307/1563000

GREENE H. W. 1983. — Dietary correlates of the origin and radiation of snakes. *American Zoologist* 23: 431-441. https://doi.org/10.1093/icb/23.2.431

HEAD J. J. & HOLROYD P. A. 2008. — Assembly and biogeography of North American Paleogene snake faunas based on an expanded fossil record. *Journal of Vertebrate Paleontology* 28: 90A.

HOFFSTETTER R. & GASC J.-P. 1969. — Vertebrae and ribs of modern reptiles, *in* GANS C. (ed.), *Biology of the Reptilia*. Vol. 1 (Morphology A). Academic Press, New York: 201-310.

HOFFSTETTER R. & RAGE J.-C. 1972. — Les *Erycinae* fossiles de France (*Serpentes*, Boidae) : compréhension et histoire de la sous-famille. *Annales de Paléontologie (Vertébrés)* 58: 82-124, pl. I-II.

HOLMAN J. A. 2000. — *Fossil Snakes of North America: Origin, Evolution, Distribution, Paleoecology*. Indiana University Press, Bloomington, Indiana, 357 p.

HOLMAN J. A., HARRISON D. L. & WARD D. J. 2006. — Late Eocene snakes from the Headon Hill Formation, southern England. *Cainozoic Research* 5: 51-62.

HOYER R. F. 1974. — Description of a Rubber Boa (*Charina bottae*) population from western Oregon. *Herpetologica* 30: 275-283. https://www.jstor.org/stable/3891834

HOYER R. F. & STEWART G. R. 2000. — Biology of the Rubber Boa (*Charina bottae*), with emphasis on *C. b. umbratica*. Part I: Capture, size, sexual dimorphism, and reproduction. *Journal of Herpetology* 34: 348-354. https://doi.org/10.2307/1565355

HSIANG A. Y., FIELD D. J., WEBSTER T. H., BEHLKE A. D. B., DAVIS M. B., RACICOT R. A. & GAUTHIER J. A. 2015. — The origin of snakes: revealing the ecology, behavior, and evolutionary history of early snakes using genomics, phenomics, and the fossil record. *BMC Evolutionary Biology* 15: 87. https://doi.org/10.1186/s12862-015-0358-5

JANDZÍK D. & BARTÍK I. 2004. — Differences in morphology of the atlas-axis complex in *Natrix natrix* and *N. tessellata* (Serpentes: Colubridae). *Biologia* 59: 219-229.

KLUGE A. G. 1993. — *Calabaria* and the phylogeny of erycine snakes. *Zoological Journal of the Linnean Society* 107: 293-351. https://doi.org/10.1111/j.1096-3642.1993.tb00290.x

LAWSON R., SLOWINSKI J. B. & BURBRINK F. T. 2004. — A molecular approach to discerning the phylogenetic placement of the enigmatic snake *Xenophidion schaeferi* among the Alethinophidia. *Journal of Zoology* 263: 285-294. https://doi.org/10.1017/S0952836904005278

LEE M. S. Y. & SCANLON J. D. 2002. — Snake phylogeny based on osteology, soft anatomy and ecology. *Biological Reviews* 77: 333-401. https://doi.org/10.1017/S1464793102005924

LENZ O. K., WILDE V., MERTZ D. F. & RIEGEL W. 2015. — New palynology-based astronomical and revised $^{40}Ar/^{39}Ar$ ages for the Eocene maar lake of Messel (Germany). *International Journal of Earth Sciences* 104: 873-889. https://doi.org/10.1007/s00531-014-1126-2

LINNAEUS C. 1758. — *Systema Naturae per Regna Tria Naturae, Secundum Classes, Ordines, Genera, Species, cum Characteribus, Differentiis, Synonymis, Locis*. Vol. 1 (10th ed.). Laurentii Salvii, Stockholm, 823 p. https://doi.org/10.5962/bhl.title.542

LONGRICH N. R., BHULLAR B.-A. S. & GAUTHIER J. A. 2012. — A transitional snake from the Late Cretaceous Period of North America. *Nature* 488: 205-208. https://doi.org/10.1038/nature11227

MAISANO J. A. & RIEPPEL O. 2007. — The skull of the Round Island Boa, *Casarea dussumieri* Schlegel, based on high-resolution X-ray computed tomography. *Journal of Morphology* 268: 371-384. https://doi.org/10.1002/jmor.10519

MATZKE N. J. & WRIGHT A. J. 2016. — Inferring node dates from tip dates in fossil Canidae: the importance of tree priors. *Biology Letters* 12: 20160328. https://doi.org/10.1098/rsbl.2016.0328

MAYR G. 2009. — *Fossil Paleogene Birds*. Springer, Heidelberg, 278 p. https://doi.org/10.1007/978-3-540-89628-9

MCDOWELL S. B. 1979. — A catalogue of the snakes of New Guinea and the Solomons, with special reference to those in the Bernice P. Bishop Museum. Part III. Boinae and Acrochordoidea (Reptilia, Serpentes). *Journal of Herpetology* 13: 1-92. https://doi.org/10.2307/1563761

MCGREW P. O., BERMAN J. E., HECHT M. K., HUMMEL J. M., SIMPSON G. G. & WOOD A. E. 1959. — The geology and paleontology of the Elk Mountain and Tabernacle Butte area, Wyoming. *Bulletin of the American Museum of Natural History* 117 (3): 121-176. http://hdl.handle.net/2246/1970

MCKENNA M. C. 1983. — Cenozoic paleogeography of North Atlantic land bridges, *in* BOTT M. H. P., SAXOV S., TALWANI M. & THIEDE J. (eds), *Structure and Development of the Greenland-Scotland Ridge: New Methods and Concepts*. Springer, Heidelberg:351-399. https://doi.org/10.1007/978-1-4613-3485-9_19

MEAD J. I. & SCHUBERT B. W. 2013. — Extinct *Pterygoboa* (Boidae, Erycinae) from the Latest Oligocene and Early Miocene of Florida. *Southeastern Naturalist* 12 (2): 427-438. https://doi.org/10.1656/058.012.0215

MOON B. R., PENNING D. A., SEGALL M. & HERREL A. 2019. — Feeding in snakes: form, function, and evolution of the feeding system, *in* BELS V. & WHISHAW I. Q. (eds), *Feeding in Vertebrates: Evolution, Morphology, Behavior, Biomechanics*. Heidelberg, Springer: 527-574. https://doi.org/10.1007/978-3-030-13739-7_14

NOONAN B. P. & CHIPPINDALE P. T. 2006. — Dispersal and vicariance: The complex evolutionary history of boid snakes. *Molecular Phylogenetics and Evolution* 40: 347-358. https://doi.org/10.1016/j.ympev.2006.03.010

NOPCSA F. B. 1923. — *Eidolosaurus* und *Pachyophis*. Zwei neue Neocom-Reptilien. *Palaeontographica* 65: 99-154.

OLORI J. C. 2010. — Digital endocasts of the cranial cavity and osseous labyrinth of the burrowing snake *Uropeltis woodmasoni* (Alethinophidia: Uropeltidae). *Copeia* 2010: 14-26. https://doi.org/10.1643/CH-09-082

OLORI J. C. & BELL C. J. 2012. — Comparative skull morphology of uropeltid snakes (Alethinophidia: Uropeltidae) with special reference to disarticulated elements and variation. *PLoS One* 7: e32450. https://doi.org/10.1371/journal.pone.0032450

OWEN R. 1850. — *Monograph on the Fossil Reptilia of the London Clay*. Part II. *Crocodilia, Ophidia*. The Palaeontographical Society, London, 68 p. + pls 1-16. https://doi.org/10.5962/bhl.title.61856

PARHAM J. F., DONOGHUE P. C. J., BELL C. J., CALWAY T. D., HEAD J. J., HOLROYD P. A., INOUE J. G., IRMIS R. B., JOYCE W. G., KSEPKA D. T., PATANÉ J. S. L., SMITH N. D., TARVER J. E., VAN TUINEN M., YANG Z. H., ANGIELCZYK K. D., GREENWOOD J. M., HIPSLEY C. A., JACOBS L. L., MAKOVICKY P. J., MÜLLER J., SMITH K. T., THEODOR J. M., WARNOCK R. C. M. & BENTON M. J. 2012. — Best practices for justifying fossil calibrations. *Systematic Biology* 61: 346-359. https://doi.org/10.1093/sysbio/syr107

PYRON R. A., BURBRINK F. T. & WIENS J. J. 2013. — A phylogeny and revised classification of Squamata, including 4161 species of lizards and snakes. *BMC Evolutionary Biology* 13: 93. https://doi.org/10.1186/1471-2148-13-93

PYRON R. A., REYNOLDS R. E. & BURBRINK F. T. 2014. — A taxonomic revision of boas (Serpentes: Boidae). *Zootaxa* 3846: 249-260. https://doi.org/10.11646/zootaxa.3846.2.5

RAGE J.-C. 1977. — An erycine snake (Boidae) of the genus *Calamagras* from the French lower Eocene, with comments on the phylogeny of the Erycinae. *Herpetologica* 33: 459-463. https://www.jstor.org/stable/3891716

RAGE J.-C. 1984. — The fossil snake *Cheilophis huerfanoensis* Gilmore, 1938, from Eocene of Colorado: Redescription and reappraisal of relationships. *Journal of Vertebrate Paleontology* 3: 219-222. https://doi.org/10.1080/02724634.1984.10011977

RAGE J.-C. 2012. — Amphibians and squamates in the Eocene of Europe: what do they tell us? *Palaeobiodiversity and Palaeoenvironments* 92: 445-457. https://doi.org/10.1007/s12549-012-0087-3

RAGE J.-C. 2013. — Mesozoic and Cenozoic squamates of Europe. *Palaeobiodiversity and Palaeoenvironments* 93: 517-534. https://doi.org/10.1007/s12549-013-0124-x

REYNOLDS R. G., NIEMILLER M. L. & REVELL L. J. 2014. — Toward a Tree-of-Life for the boas and pythons: Multilocus species-level phylogeny with unprecedented taxon sampling. *Molecular Phylogenetics and Evolution* 71: 201-213. https://doi.org/10.1016/j.ympev.2013.11.011

RIEPPEL O. 1978a. — A functional and phylogenetic interpretation of the skull of the Erycinae (Reptilia, Serpentes). *Journal of Zoology* 186: 185-208. https://doi.org/10.1111/j.1469-7998.1978.tb03365.x

RIEPPEL O. 1978b. — The evolution of the naso-frontal joint in snakes and its bearing on snake origins. *Zeitschrift für zoologische Systematik und Evolutionsforschung* 16: 14-27. https://doi.org/10.1111/j.1439-0469.1978.tb00917.x

RIEPPEL O. & ZAHER H. 2002. — The skull of the Uropeltinae (Reptilia, Serpentes), with special reference to the otico-occipital region. *Bulletin of the Natural History Museum, London (Zoology)* 68: 123-130.

ROMER A. S. 1956. — *Osteology of the Reptiles*. University of Chicago Press, Chicago, 772 p.

RONQUIST F., TESLENKO M., VAN DER MARK P., AYRES D. L., DARLING A., HÖHNA S., LARGET B., LIU L., SUCHARD M. A. & HUELSENBECK J. P. 2012. — MrBayes 3.2: efficient Bayesian phylogenetic inference and model choice across a large model space. *Systematic Biology* 61: 539-542. https://doi.org/10.1093/sysbio/sys029

ROSE K. D. 2012. — The importance of Messel for interpreting Eocene Holarctic mammalian faunas. *Palaeobiodiversity and Palaeoenvironments* 92: 631-647. https://doi.org/10.1007/s12549-012-0090-8

SAVAGE D. E. & RUSSELL D. E. 1977. — Comments on mammalian paleontologic stratigraphy and geochronology; Eocene stages and mammal ages of Europe and North America. *Geobios, Mémoire spécial* 1: 47-56. https://doi.org/10.1016/S0016-6995(77)80006-5

SCANFERLA C. A. 2016. — Postnatal ontogeny and the evolution of macrostomy in snakes. *Royal Society Open Science* 3: 160612. https://doi.org/10.1098/rsos.160612

SCANFERLA C. A., SMITH K. T. & SCHAAL S. F. K. 2016. — Revision of the cranial anatomy and phylogenetic relationships of the Eocene minute boas *Messelophis variatus* and *Messelophis ermannorum* (Serpentes, Booidea). *Zoological Journal of the Linnean Society* 176: 182-206. https://doi.org/10.1111/zoj.12300

SCHAAL S. 2004. — *Palaeopython fischeri* n. sp. (Serpentes: Boidae), eine Riesenschlange aus dem Eozän (MP 11) von Messel. *Courier Forschungsinstitut Senckenberg* 252: 35-45.

SEUFER H. 2001. — Kleine Riesenschlangen. Pflege und Zucht von Sandboas im Terrarium. *Draco (Münster)* 5: 56-67.

SMITH K. T. 2009a. — A new lizard assemblage from the earliest Eocene (zone Wa0) of the Bighorn Basin, Wyoming, USA: Biogeography during the warmest interval of the Cenozoic. *Journal of Systematic Palaeontology* 7: 299-358. https://doi.org/10.1017/S1477201909002752

SMITH K. T. 2009b. — Eocene lizards of the clade *Geiseltaliellus* from Messel and Geiseltal, Germany, and the early radiation of Iguanidae (Squamata: Iguania). *Bulletin of the Peabody Museum of Natural History* 50: 219-306. https://doi.org/10.3374/014.050.0201

SMITH K.T. 2011. — The long-term history of dispersal among lizards in the early Eocene: New evidence from a microvertebrate assemblage in the Bighorn Basin of Wyoming, U.S.A. *Palaeontology* 54 (6): 1243-1270. https://doi.org/10.1111/j.1475-4983.2011.01107.x

SMITH K. T. 2013. — New constraints on the evolution of the snake clades Ungaliophiinae, Loxocemidae and Colubridae (Serpentes), with comments on the fossil history of erycine boids in North America. *Zoologischer Anzeiger* 252: 157-182. https://doi.org/10.1016/j.jcz.2012.05.006

SMITH K. T. 2017. — First crocodile-tailed lizard (Squamata: *Pan-Shinisaurus*) from the Paleogene of Europe. *Journal of Vertebrate Paleontology* 37: e1313743. https://doi.org/10.1080/02724634.2017.1313743

SMITH K. T. & GAUTHIER J. A. 2013. — Early Eocene lizards of the Wasatch Formation near Bitter Creek, Wyoming: diversity and paleoenvironment during an interval of global warming. *Bulletin of the Peabody Museum of Natural History* 54: 135-230. https://doi.org/10.3374/014.054.0205

SMITH K. T. & SCANFERLA A. 2016. — Fossil snake preserving three trophic levels and evidence for an ontogenetic dietary shift. *Palaeobiodiversity and Palaeoenvironments* 96: 589-599. https://doi.org/10.1007/s12549-016-0244-1

SMITH K.T., SCHAAL S., SUN W. & LI C.T. 2011. — Acrodont iguanians (Squamata) from the middle Eocene of the Huadian Basin of Jilin Province, China, with a critique of the taxon "Tinosaurus". *Vertebrata PalAsiatica* 49 (1): 69-84.

SMITH K. T., SCHAAL S. F. K. & HABERSETZER J. 2018. — *Messel: An Ancient Greenhouse Ecosystem*. Schweizerbart, Stuttgart, 355 p.

SOOD M. S. 1941. — The caudal vertebræ of *Eryx johnii* (Russell). *Proceedings of the Indian Academy of Sciences B* 14: 390-394. https://doi.org/10.1007/BF03051150

STADLER T. 2010. — Sampling-through-time in birth-death trees. *Journal of Theoretical Biology* 267: 396-404. https://doi.org/10.1016/j.jtbi.2010.09.010

STEBBINS R. C. 2003. — *A Field Guide to Western Reptiles and Amphibians*. Houghton Mifflin, New York, 533 p.

SWOFFORD D. L. 2003. — PAUP*: Phylogenetic Analysis Using Parsimony (* and Other Methods). Version 4.

SZYNDLAR Z. 1994. — Oligocene snakes of southern Germany. *Journal of Vertebrate Paleontology* 14: 24-37. https://doi.org/10.1080/02724634.1994.10011536

SZYNDLAR Z. & RAGE J.-C. 2003. — *Non-erycine Booidea from the Oligocene and Miocene of Europe*. Polish Academy of Sciences, Krakow, 109 p.

UNDERWOOD G. 1976. — A systematic analysis of boid snakes, *in* BELLAIRS A. D. A. & COX C. B. (eds), *Morphology and Biology of Reptiles*. Academic Press, London: 151-176 (Linnean Society Symposium Series Number 3).

VIDAL N., DELMAS A.-S. & HEDGES S. B. 2007. — The higher-level relationships of alethinophidian snakes inferred from seven nuclear and mitochondrial genes, *in* HENDERSON R. W. & POWELL R. (eds), *Biology of the Boas and Pythons*. Eagle Mountain Publishing, Eagle Mountain: 27-33.

VIDAL N., MARIN J., SASSI J., BATTISTUZZI F. U., DONNELLAN S., FITCH A. J., FRY B. G., VONK F. J., RODRIGUEZ DE LA VEGA R. C., COULOUX A. & HEDGES S. B. 2012. — Molecular evidence for an Asian origin of monitor lizards followed by Tertiary dispersals to Africa and Australasia. *Biology Letters* 8: 853-855. https://doi.org/10.1098/rsbl.2012.0460

WEBER J. 1991. — Untersuchungen zur Tonmineralführung der Messel-Formation in der Fundstätte Messel (Mittel-Eozän). *Courier Forschungsinstitut Senckenberg* 139: 71-81.

WILCOX T. P., ZWICKL D. J., HEATH T. A. & HILLIS D. M. 2002. — Phylogenetic relationships of the dwarf boas and a comparison of Bayesian and bootstrap measures of phylogenetic support. *Molecular Phylogenetics and Evolution* 25: 361-371. https://doi.org/10.1016/S1055-7903(02)00244-0

YI H.-Y. & NORELL M. A. 2015. — The burrowing origin of modern snakes. *Science Advances* 1: e1500743. https://doi.org/10.1126/sciadv.1500743

ZEROVA G. A. 1989. — The first find of a fossil sand boa of the genus *Albaneryx* (Serpentes, Boidae) in the USSR. *Vestnik Zoologii* 1989: 30-35.

ZHANG C., STADLER T., KLOPFSTEIN S., HEATH T. A. & RONQUIST F. 2016. — Total-evidence dating under the fossilized birth-death process. *Systematic Biology* 65: 228-249. https://doi.org/10.1093/sysbio/syv080

Submitted on 29 May 2019;
accepted on 8 November 2019;
published on 14 January 2021.

APPENDIX 1. — Supplementary material, Figures S1 to S17. Abbreviations: **ATV**, Anterior trunk vertebra; **PTV**, Posterior trunk vertebra.

S1: Skull:	https://sciencepress.mnhn.fr/sites/default/files/documents/fr/g2021v43a1-s1-skull.pdf
S2: Maxilla:	https://sciencepress.mnhn.fr/sites/default/files/documents/fr/g2021v43a1-s2-maxilla.pdf
S3: Nasal:	https://sciencepress.mnhn.fr/sites/default/files/documents/fr/g2021v43a1-s3-nasal.pdf
S4: Prefrontal:	https://sciencepress.mnhn.fr/sites/default/files/documents/fr/g2021v43a1-s4-prefrontal.pdf
S5: Frontal:	https://sciencepress.mnhn.fr/sites/default/files/documents/fr/g2021v43a1-s5-frontal.pdf
S6: Postorbital:	https://sciencepress.mnhn.fr/sites/default/files/documents/fr/g2021v43a1-s6-postorbital.pdf
S7: Parabasisphenoid:	https://sciencepress.mnhn.fr/sites/default/files/documents/fr/g2021v43a1-s7-parabasisphenoid.pdf
S8: Supratemporal:	https://sciencepress.mnhn.fr/sites/default/files/documents/fr/g2021v43a1-s8-supratemporal.pdf
S9: Quadrate:	https://sciencepress.mnhn.fr/sites/default/files/documents/fr/g2021v43a1-s9-quadrate.pdf
S10: L. Pterygoid:	https://sciencepress.mnhn.fr/sites/default/files/documents/fr/g2021v43a1-s10-pterygoidl.pdf
S11: R. Pterygoid:	https://sciencepress.mnhn.fr/sites/default/files/documents/fr/g2021v43a1-s11-pterygoidr.pdf
S12: Ectopterygoid:	https://sciencepress.mnhn.fr/sites/default/files/documents/fr/g2021v43a1-s12-ectopterygoid.pdf
S13: Dentary:	https://sciencepress.mnhn.fr/sites/default/files/documents/fr/g2021v43a1-s13-dentary.pdf
S14: Compound bone:	https://sciencepress.mnhn.fr/sites/default/files/documents/fr/g2021v43a1-s14-compound_bone.pdf
S15: ATV:	https://sciencepress.mnhn.fr/sites/default/files/documents/fr/g2021v43a1-s15-atv.pdf
S16: PTV:	https://sciencepress.mnhn.fr/sites/default/files/documents/fr/g2021v43a1-s16-ptv.pdf
S17: Tail:	https://sciencepress.mnhn.fr/sites/default/files/documents/fr/g2021v43a1-s17-tail.pdf

APPENDIX 2. — Supplementary material, NEX Matrices.

Character-taxon matrix with MrBayes script:

https://sciencepress.mnhn.fr/sites/default/files/documents/fr/g2021v43a1-s18-rageryx_bi_fbd_fin.nex

Character-taxon matrix with character descriptions for use in PAUP:

https://sciencepress.mnhn.fr/sites/default/files/documents/fr/g2021v43a1-s19-rageryx_mp_fin.nex